AD-A044 742 REGIS COLL RESEARCH CENTER WESTON MASS F/G 22/2
DEVELOPMENT AND APPLICATION OF ELECTRICAL AND MECHANICAL PROTOT--ETC(U)
MAY 77 M AHMED, P B ANDERSON, W J BURKE F19628-75-C-0081
UNCLASSIFIED AFGL-TR-77-0119 NL

1 OF 1
AD A044742

END
DATE FILMED
10-77
DDC

12

AFGL-TR-77-0119

DEVELOPMENT AND APPLICATION OF ELECTRICAL AND MECHANICAL PROTOTYPE INSTRUMENTS FOR SPACE ENVIRONMENT STUDIES

Mukhtar Ahmed
Peter B. Anderson
William J. Burke
Frederick J. Rich

Regis College Research Center
235 Wellesley Street
Weston, Massachusetts 02193

31 May 1977

Final Report for Period 16 February 1975 - 30 April 1977

Approved for public release; distribution unlimited

AIR FORCE GEOPHYSICS LABORATORY
AIR FORCE SYSTEMS COMMAND
UNITED STATES AIR FORCE
HANSCOM AFB, MASSACHUSETTS 01731

SECURITY CLASSIFICATION OF THIS PAGE (When Data Entered)

REPORT DOCUMENTATION PAGE

READ INSTRUCTIONS BEFORE COMPLETING FORM

1. REPORT NUMBER: AFGL-TR-77-0119	2. GOVT ACCESSION NO.
3. RECIPIENT'S CATALOG NUMBER	
4. TITLE (and Subtitle): DEVELOPMENT AND APPLICATION OF ELECTRICAL AND MECHANICAL PROTOTYPE INSTRUMENTS FOR SPACE ENVIRONMENT STUDIES	5. TYPE OF REPORT & PERIOD COVERED: FINAL REPORT, 16 FEB 75 — 30 APR 77
	6. PERFORMING ORG. REPORT NUMBER
7. AUTHOR(s): Mukhtar Ahmed, Peter B. Anderson, William J. Burke, Frederick J. Rich	8. CONTRACT OR GRANT NUMBER(s): F19628-75-C-0081
9. PERFORMING ORGANIZATION NAME AND ADDRESS: Regis College, 235 Wellesley Street, Weston, Massachusetts 02193	10. PROGRAM ELEMENT, PROJECT, TASK AREA & WORK UNIT NUMBERS: 61102F, 2311G202, G2
11. CONTROLLING OFFICE NAME AND ADDRESS: Air Force Geophysics Laboratory, Hanscom AFB, Massachusetts 01731, Contract Monitor/Susan C. Bredesen, PHR	12. REPORT DATE: 31 May 1977
	13. NUMBER OF PAGES: 93
14. MONITORING AGENCY NAME & ADDRESS (if different from Controlling Office): 95p.	15. SECURITY CLASS. (of this report): Unclassified
	15a. DECLASSIFICATION/DOWNGRADING SCHEDULE

16. DISTRIBUTION STATEMENT (of this Report)

APPROVED FOR PUBLIC RELEASE, DISTRIBUTION UNLIMITED

17. DISTRIBUTION STATEMENT (of the abstract entered in Block 20, if different from Report)

18. SUPPLEMENTARY NOTES

19. KEY WORDS (Continue on reverse side if necessary and identify by block number)

AEOLUS	electric field	ionization
auroral oval	electron probe	ionosphere
conjugate photoelectrons	electrons	ions
density	flux	inverted V precipitation
DMSP	INJUN 5	ISIS 1

20. ABSTRACT (Continue on reverse side if necessary and identify by block number)

The objectives of this contract have been adequately realized. The development, calibration and integration of the prototype instrumentation were applied in scientific experiments flown on two AEOLUS rocket payloads, which involved circuit design, printed circuit layouts, electronic density package design, and electronics package design. Analysis and synthesis of flight results involved plasma measurements including bulk ion motions, energy distributions, plasma diagnostic sensors, physical dimensions and location under changing geophysical conditions.

DD FORM 1 JAN 73 1473 EDITION OF 1 NOV 65 IS OBSOLETE Unclassified

SECURITY CLASSIFICATION OF THIS PAGE (When Data Entered)

19. Key words (Continued)

non-Maxwellian	polar wind	scintillation
parabolic ionization	S3-2	sweep/calibration
plasma	S3-3	temperature
plasmapause	SAR arc	trough
polar cap	SCATHA	vehicle potential

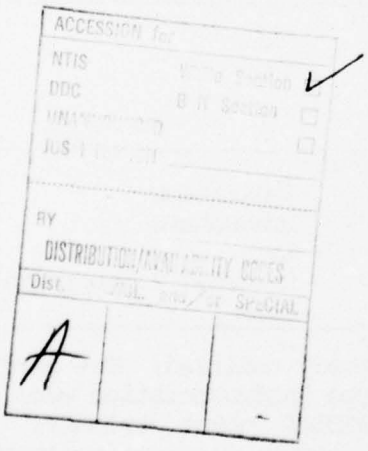

Table of Contents

MID-LATITUDE TROUGH PHENOMENON, SCINTILLATION, AURORAL OVAL, IONOSPHERIC MODELS FROM THE F_2 PEAK TO 1000 km

MUKHTAR AHMED

1. INTRODUCTION

A knowledge of the characteristics and physical processes operating in the environment of space satellites-Topside Ionosphere, Plasmasphere, and Magnetosphere is very important, especially the ionization irregularities as they affect HF radio propagation. Hence, an extensive investigation to understand the factors governing the production, location, fine structure and morphology of ionospheric features like

(a) Mid-latitude trough phenomenon

(b) Scintillation phenomenon

(c) Auroral oval

(d) Development of ionospheric models from the F_2 peak to 1000 km in Ionospheric Monitoring work

was undertaken. The results of this work are expected to provide much needed inputs to the development and design of advanced systems for reliable global communications such as AFSATCOM and others.

We shall discuss below the different investigations in detail.

2. MID-LATITUDE TROUGH

This ionospheric phenomena occurs in the region of steep ionization gradients-an important region for radar back sector work needed for routine monitoring and surveillance. A detailed knowledge of this phenomenon, especially its physical dimensions under differing geophysical conditions, is still in a rudimentary stage. We seek to make contributions in this regard.

This study of the morphology of several features of the main trough is based on five years' data obtained from thermal plasma sensors flown on the ISIS-I and INJUN-V satellites. Boom-mounted spherical electrostatic

analyzers were biased to measure positive ions on ISIS-I and electrons on INJUN V. The dayside trough is also examined and the trough structure, that is, its width, depth, equatorial and poleward gradients are determined as a function of local time and season, for Kp $\leq$ 3. Additional plasma depletions observed on the dayside between L = 2 and 4 at altitudes greater that 1500 km are also described.

The main trough is a region where thermal plasma density depletions are consistently observed at mid-latitudes in the nightside ionosphere. It is considered to indicate the boundary between regions of the ionosphere having different primary source processes: firstly, the low latitude ionosphere or plasmasphere, resulting principally from solar radiation, and secondly, a high latitude region due primarily to magnetospheric particle precipitation.

2.1 METHOD

In Figure 1, the orbital parameters for the satellites utilized are given. Approximately 12,000 whole or partial orbits of ISIS-I data and nearly 5,000 orbits of INJUN-V data acquired globally were examined.

A representative trough obtained on ISIS-I (orbit 6864) is shown in Figure 2. It is shown to define the properties we have measured.

The equatorial edge of the trough, point a, is the location of the intercept of lines drawn through the first ionization maximum in the precipitation region, and the poleward trough wall. The poleward edge of the trough is at point d.

The width is taken to be the invariant latitude range between points a and d.

The depth of the trough is defined for both its equatorial and poleward

ORBITAL PARAMETERS

SATELLITE	APOGEE (Km)	PERIGEE (Km)	INCLINATION
ISIS - I	3526	525	88.5°
INJUN - V	2526	666	80.7°

Figure 1. Orbital parameters for the ISIS I and INJUN V satellites

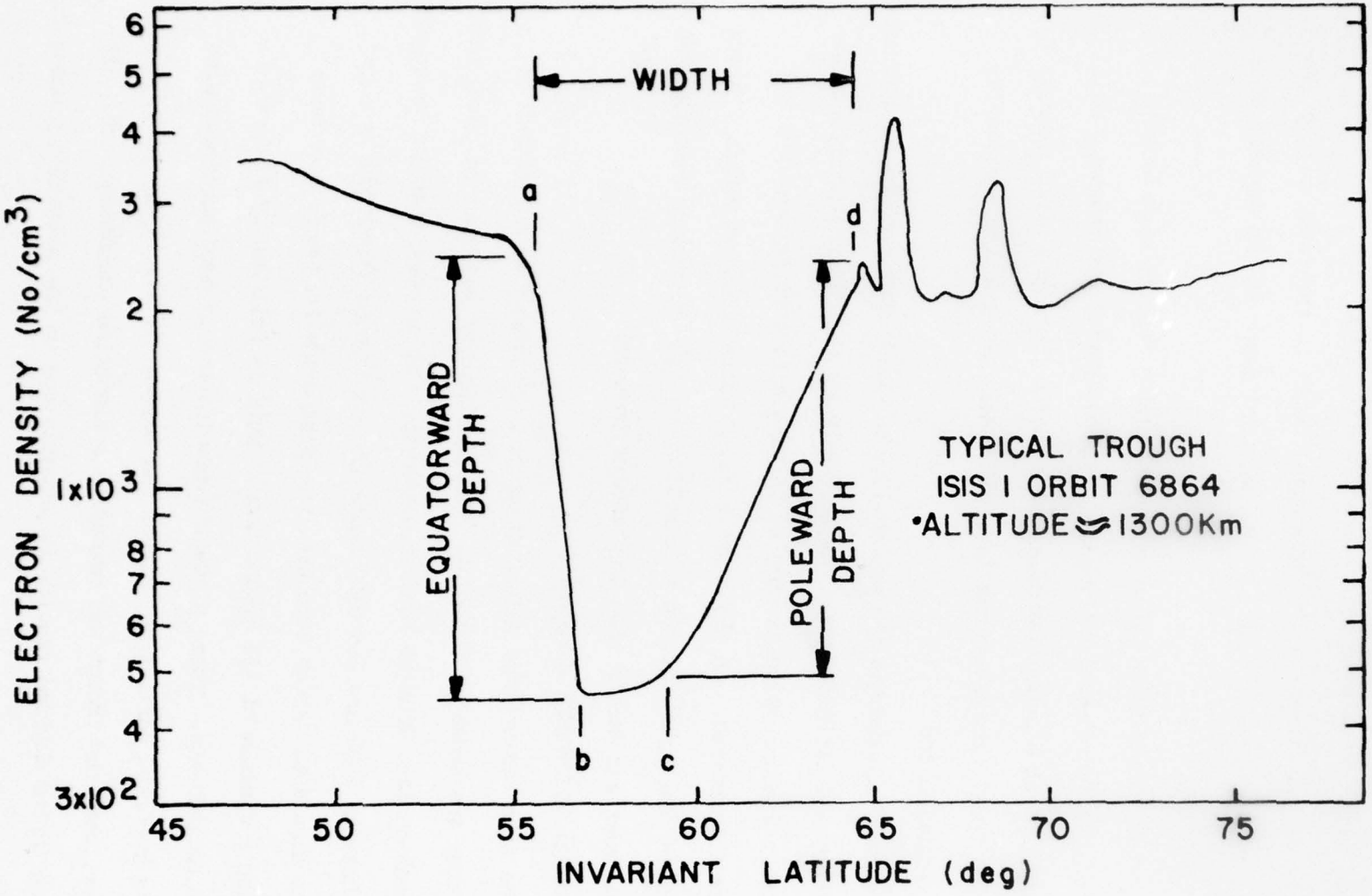

Figure 2. Typical trough, ISIS I, Orbit 6864, altitude 1300 km

edge since the densities at points a and d and at the base b and c are frequently very different. The equatorial depth is the ratio of the density at a over the density at b. The poleward depth is the density at d over the density at c.

In order to minimize the effects of varying density with height, normalized gradients were evaluated at the equatorial and poleward wall. Then the gradient at the equatorial edge is the density a minus density b divided by the latitude a minus latitude b all over the average density between points a and b.

Figure 3 illustrates the variability of individual troughs at different local times and altitudes. On the left side of the figure, troughs measured within 2 hours of local noon at varying altitudes between 600 and 2300 are illustrated. On the right side, results obtained within 2 hours of midnight are given for 600 km and 3500 km. The nightside troughs tend to be broader and deeper than the dayside troughs.

2.2 TROUGH OCCURRENCE FREQUENCY

The first quantitive values of trough occurrence as a function of local time are shown in Figure 4. The results for each hour of local time are based on data from at least two seasons. It is seen that in the night hours between 1900 hrs and 0400 hours the occurrence frequency is high, greater than 95%. After 0400 hrs, the occurrence frequency decreases reaching a minimum of 48% around noon. This is followed by a steady increase to 1900 hrs. These nighttime results are in good agreement with results reported earlier by Tulunay and Sayers (1971). They concluded, however, that the trough was primarily a nighttime phenomenon. The difference in the daytime results is probably due to the selection process for

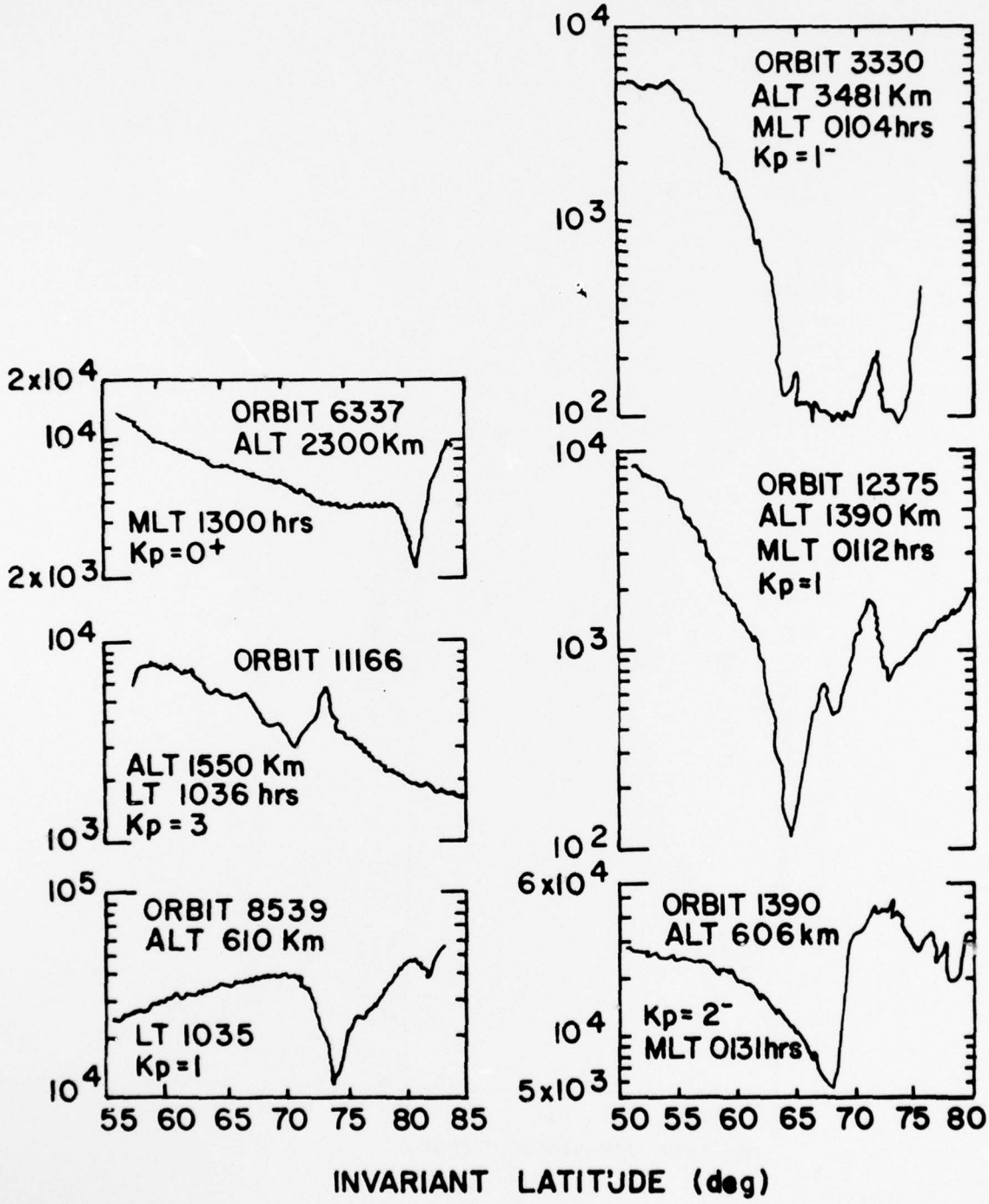

Figure 3. Variability of troughs at different local times and altitudes, ISIS I

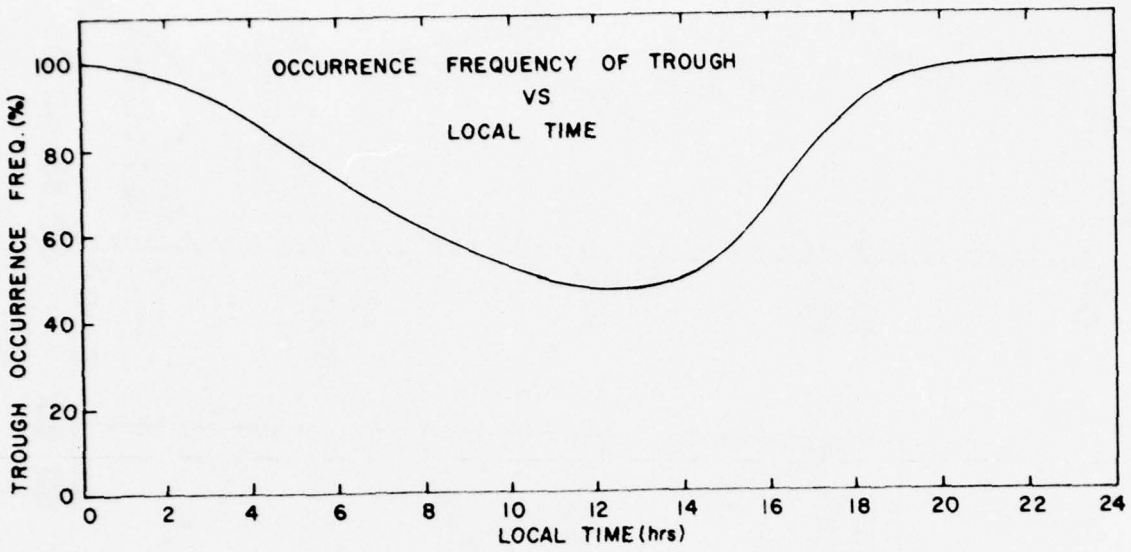

Figure 4. Occurrence frequency of trough vs local time

each study. Tulunay and Sayers used the criterion that the ratio of the maximum to minimum density in the trough must be greater than 2:1 for a trough to be noted. It will be seen from our results on trough amplitude in Figure 9 that this criterion would eliminate most of the midday troughs which we have identified, where values as low as 1.25:1 are identified.

2.3 TROUGH LOCATION

The mean location of the equatorial edge of the trough as a function of time is shown for the four seasons in Figure 5. It is seen on the polar plot that the seasonal variation of the trough position at a given local time is small as indicated on the figure except for the hours between 6 and 9 am. In the summer the invariant latitude and hence the L value of the trough increases steadily between 0400 and 1000 hrs. In the winter, the trough position remains close to the nighttime value of about 60° invariant latitude up to 0900 hours. This is followed by a rapid increase between 0900 and 1000 hrs. These differences are considered to be due to the varying tilt angle of the sun with season.

The high L value (72° invariant latitude) of the trough on the dayside near local noon should be noted. During the daytime the trough is found at the equatorial edge of the cleft precipitation region. At night it is found at the equatorial edge of the auroral precipitation region.

2.4 TROUGH WIDTH

The first systematic study of trough width is presented in Figure 6. The trough width exhibits a simple diurnal variation with a maximum of $7\text{-}12^{\circ}$ between 0300 and 0500 hours and a minimum of about 4° around local noon. It then increases gradually to the early morning maximum. There is a pronounced seasonal variation in the night hours. For example, at

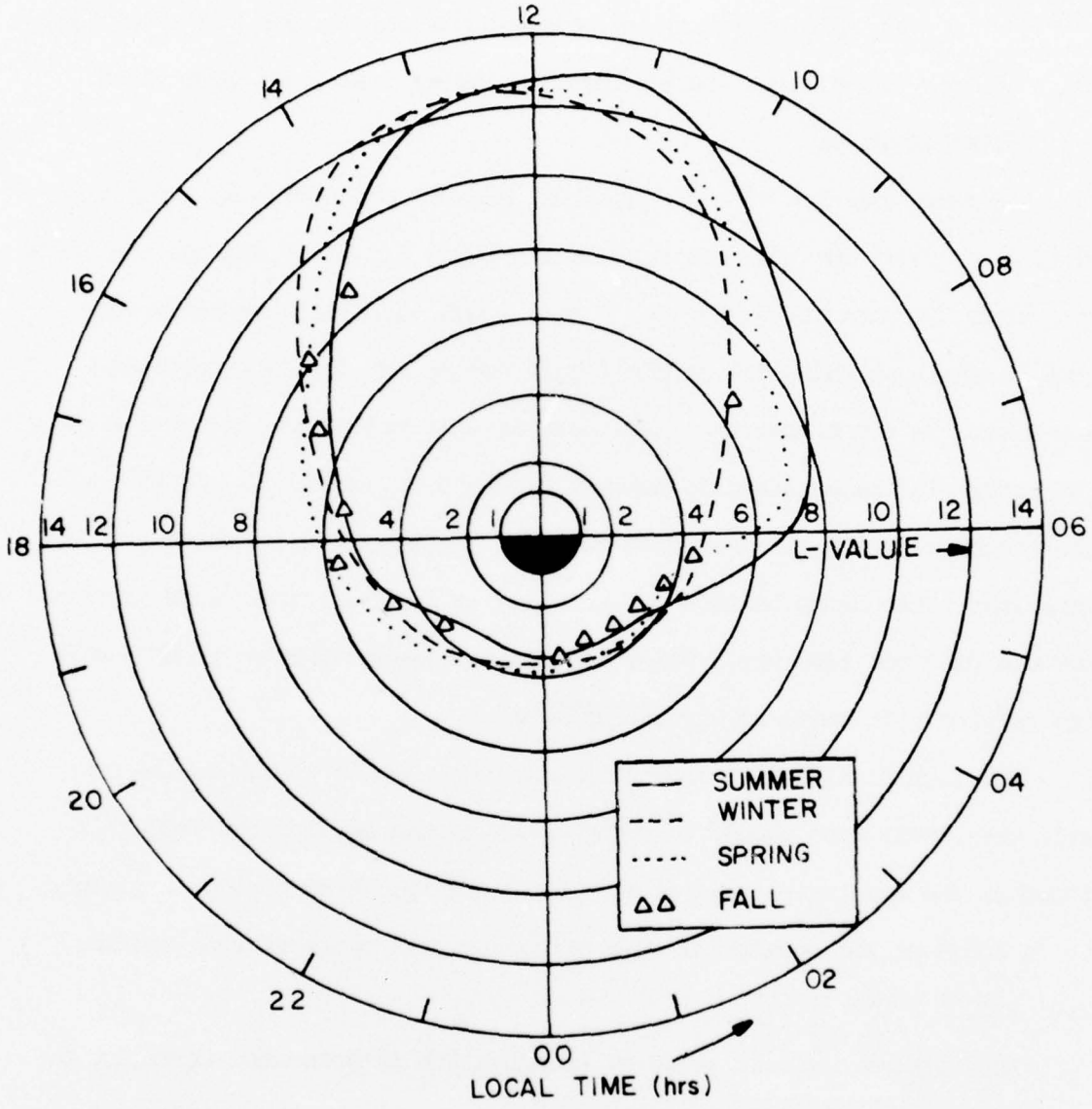

Figure 5. Mean location of equatorial edge of the trough as a function of local time, L value, and season

0500 hours the width is nearly 12^{o} in winter and 5^{o} in summer. Spring and fall values lie between these limits. The strong influence of solar radiation on the width is evident from the onset times of the rapid decrease in width in the morning hours of each season.

The standard deviations for all trough parameters are large as illustrated in Figure 6 where the mean width data for summer and winter is given with calculated standard deviation. The deviation in width is approximately $\pm 2^{o}$. We have searched for factors contributing to the standard deviation, including altitude, Kp, previous magnetic history. In the statistical analysis of data, the altitudes of trough observations used in any hour of local time were found to be quite considerable and were suspected as one of the major causes of large standard deviation. Figure 7 shows a plot variation of trough width against altitude. This is an important result. This is further confirmed by a comparison of simultaneous measurements of ion densities from our SEA experiment on ISIS-I and the topside ionosonde on ISIS-II, kindly provided by Dr. Whitteker of Canadian Department of Communications, Ottawa, Canada, shown in Figure 8.

2.5 TROUGH DEPTH

The depth of amplitude of the trough, that is, the ratio of the plasma density at the trough edge to the value at the base of the trough wall, has been evaluated for both poleward and equatorial edges. It is seen in Figure 9 that the amplitude is a minimum around local noon and a maximum near midnight. The depth changes by a factor of 10 throughout the day in winter and by a factor of 2.3 in summer. The results for spring and fall lie between these limits.

Similar results were obtained for the amplitude at the poleward edge

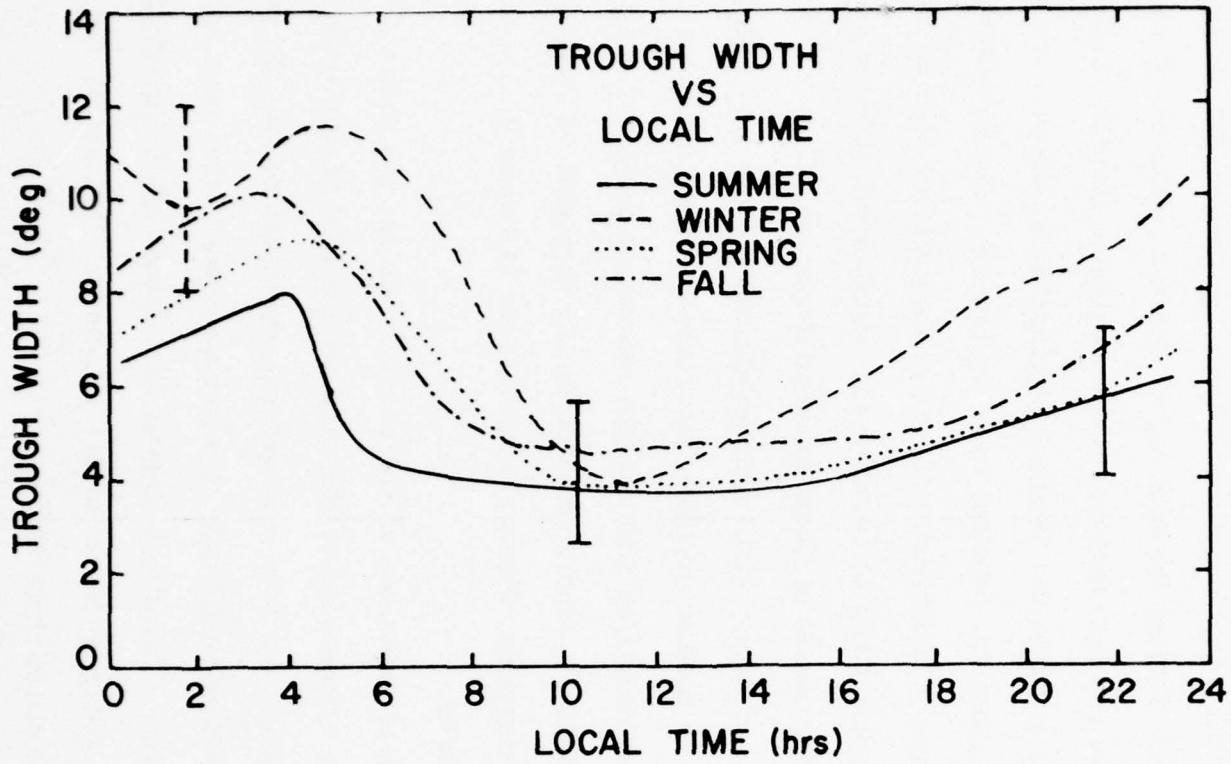

Figure 6. Trough width vs local time

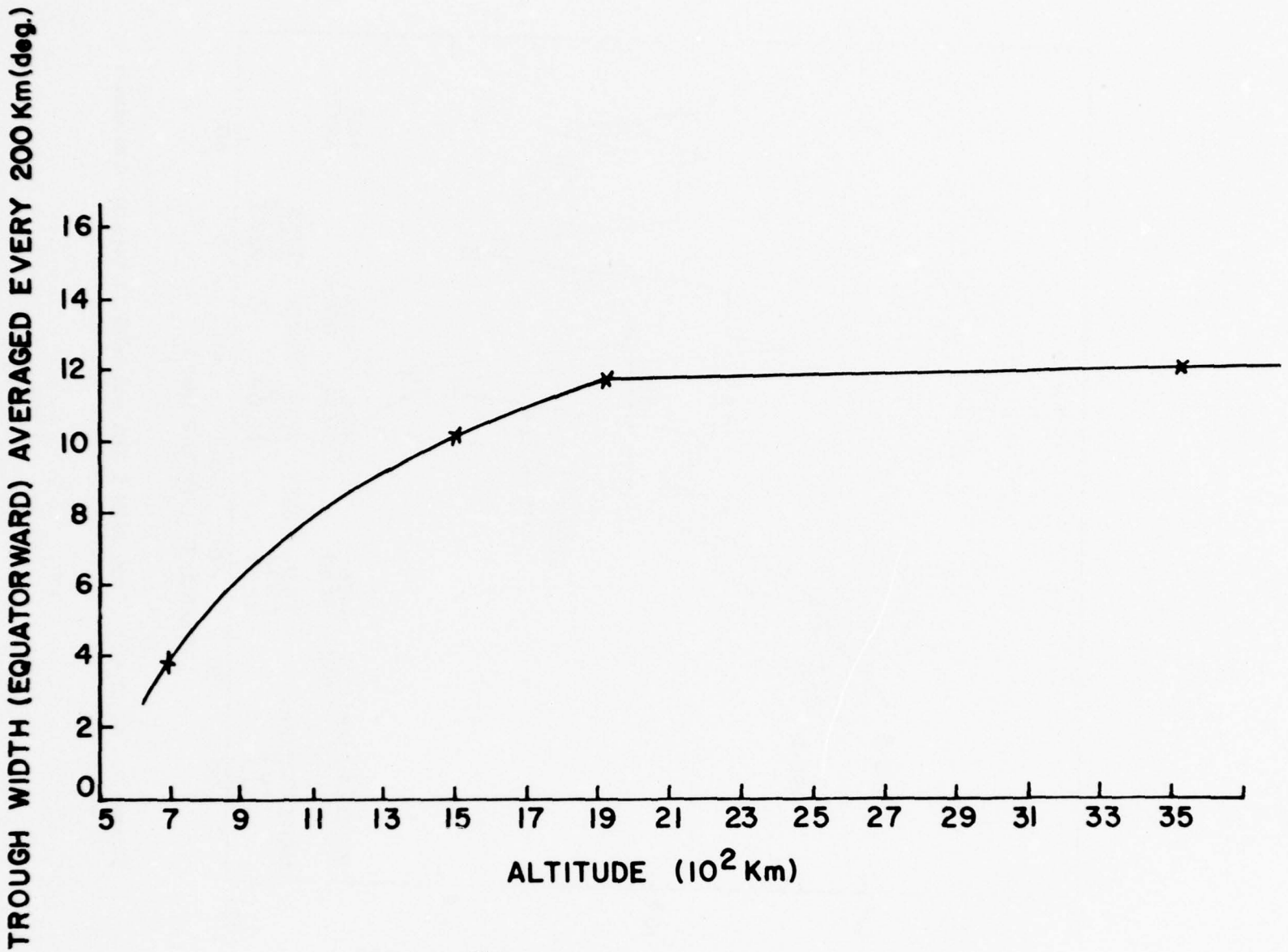

Figure 7. Trough width vs altitude

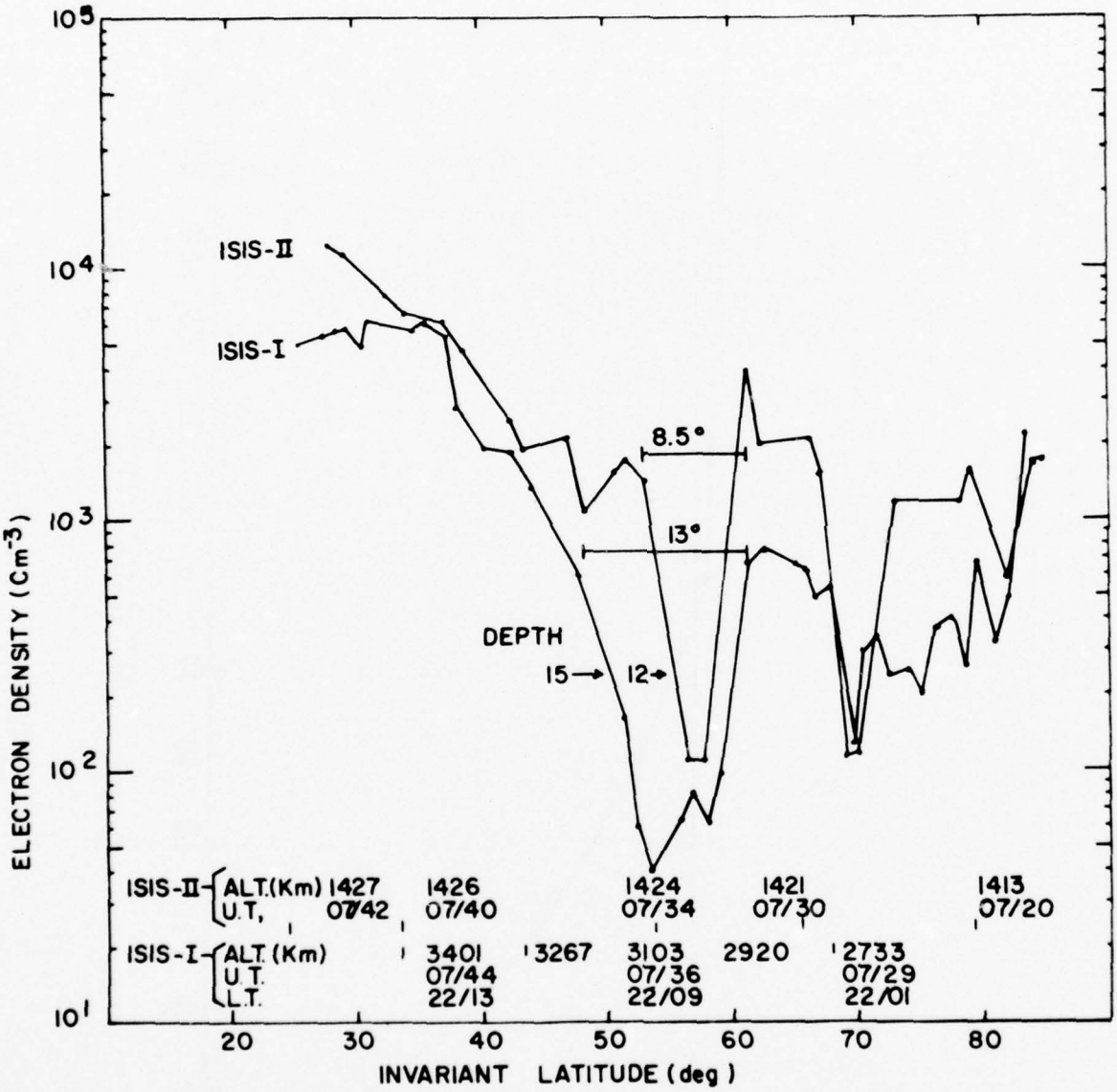

Figure 8. Ne in-situ from ISIS I SEA and ISIS II Topside ionosonde

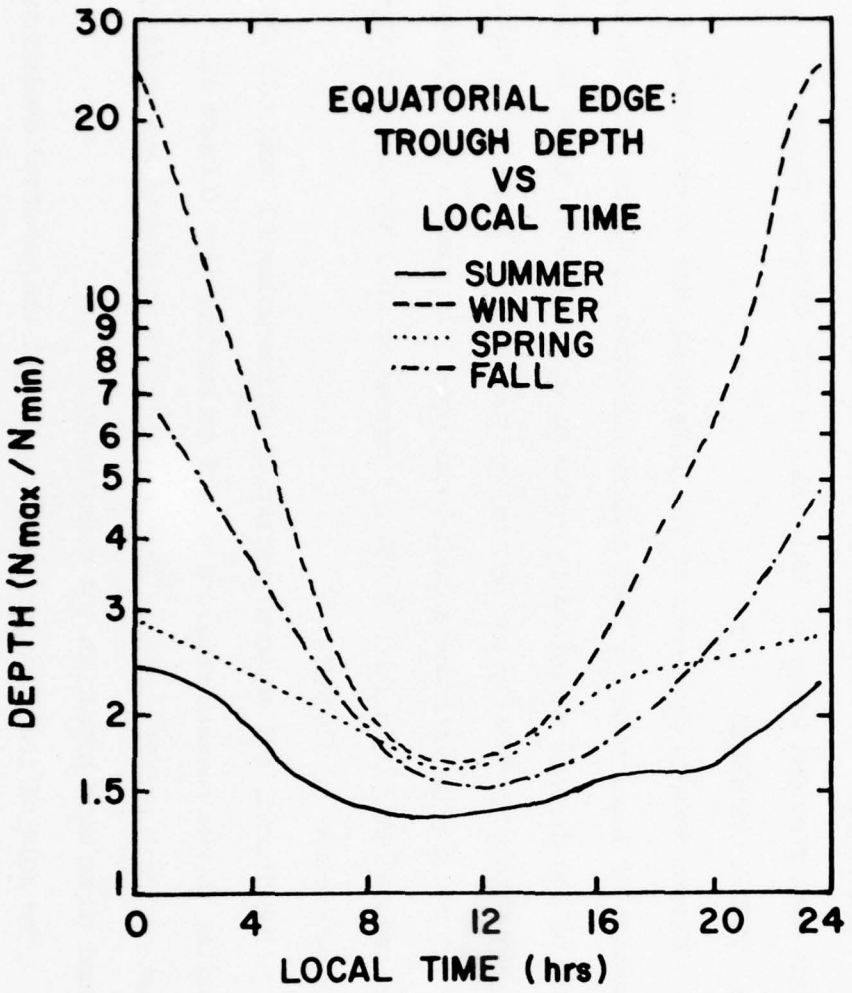

Figure 9. Equatorial edge trough depth vs local time

with the exception of winter nights when the ratios were 2 to 3 times smaller than for the equatorial depth. This reflects primarily the smaller contribution of solar radiation to the ionization in the polar regions on winter nights. The altitude variation was suspected here as a major cause of standard deviation in trough depth. This was investigated by examining the variation in trough depths in data from a narrow local time sector but showing a wide variation in altitude. Figure 10 shows trough depth plotted against altitude. Confirmation of this was observed in the topside ionosonde data provided us by Dr. Whitteker of CRC, Ottawa, Canada.

2.6 TROUGH GRADIENTS

Plasma density gradients at the equatorial edge of the trough as a function of local time for each season are shown in Figure 11. The amplitude of the diurnal variation is greatest in winter when there is observed an 80% change in density per degree latitude at 2000 hours and a minimum of 25% per degree latitude around local noon. In summer, the gradients are reduced with a maximum of 45% per degree at 2000 hrs and a minimum of 17% per degree at 1300 hrs.

The diurnal and seasonal variation of the poleward gradients are similar to the results obtained at the equatorial edge (Figure 12). The most noticeable difference is that the poleward gradients are consistently found to be much higher in the night hours.

The role of the altitude variation toward the standard deviation in the results was investigated by examining the equatorward and poleward gradient in an hour of local time as shown in Figure 13.

A regression analysis performed for the equatorward and poleward gradients shows the following: Trough equatorward gradient $(\frac{1}{N}\frac{dN}{d\Lambda})$ =

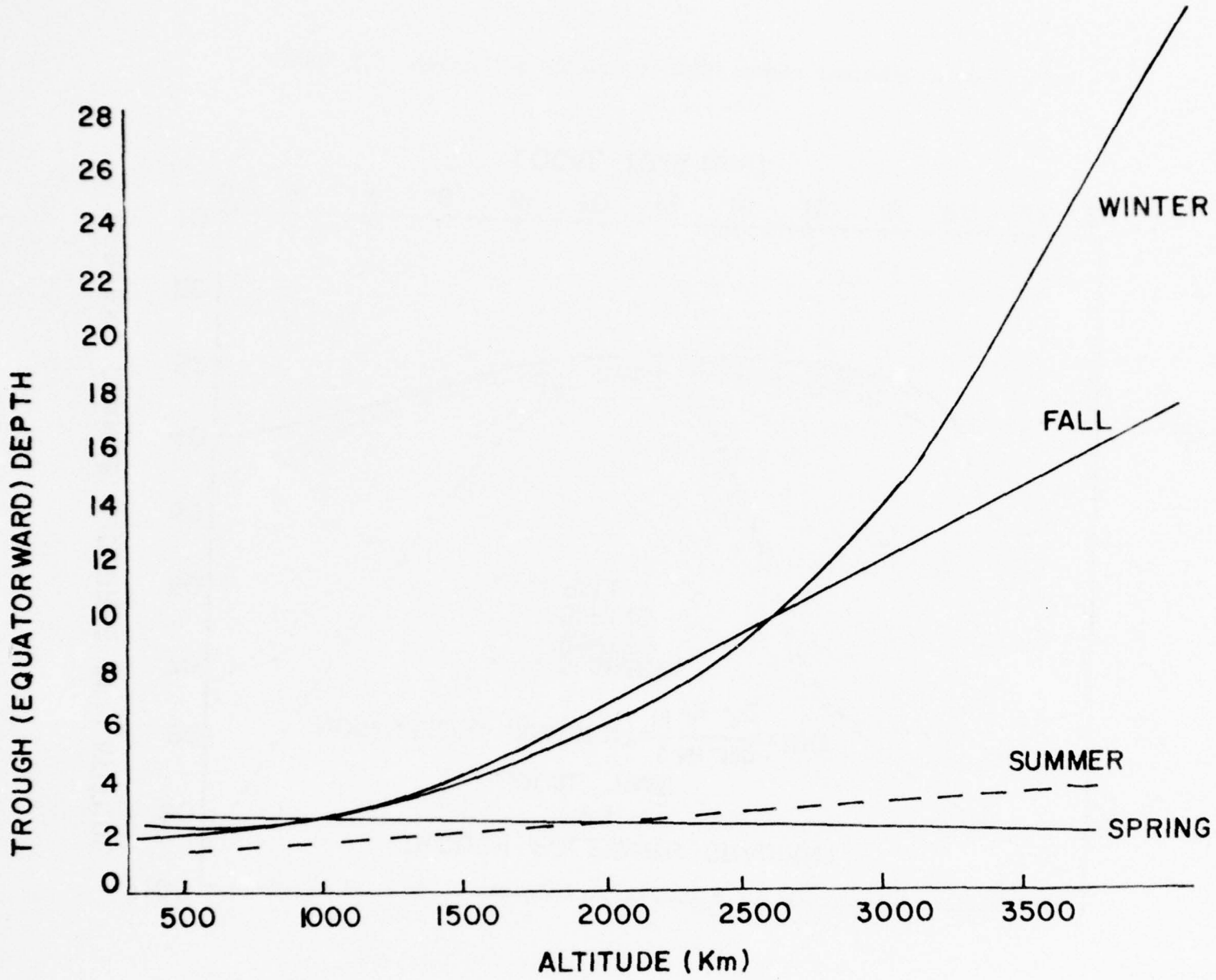

Figure 10. Equatorial edge trough depth vs altitude

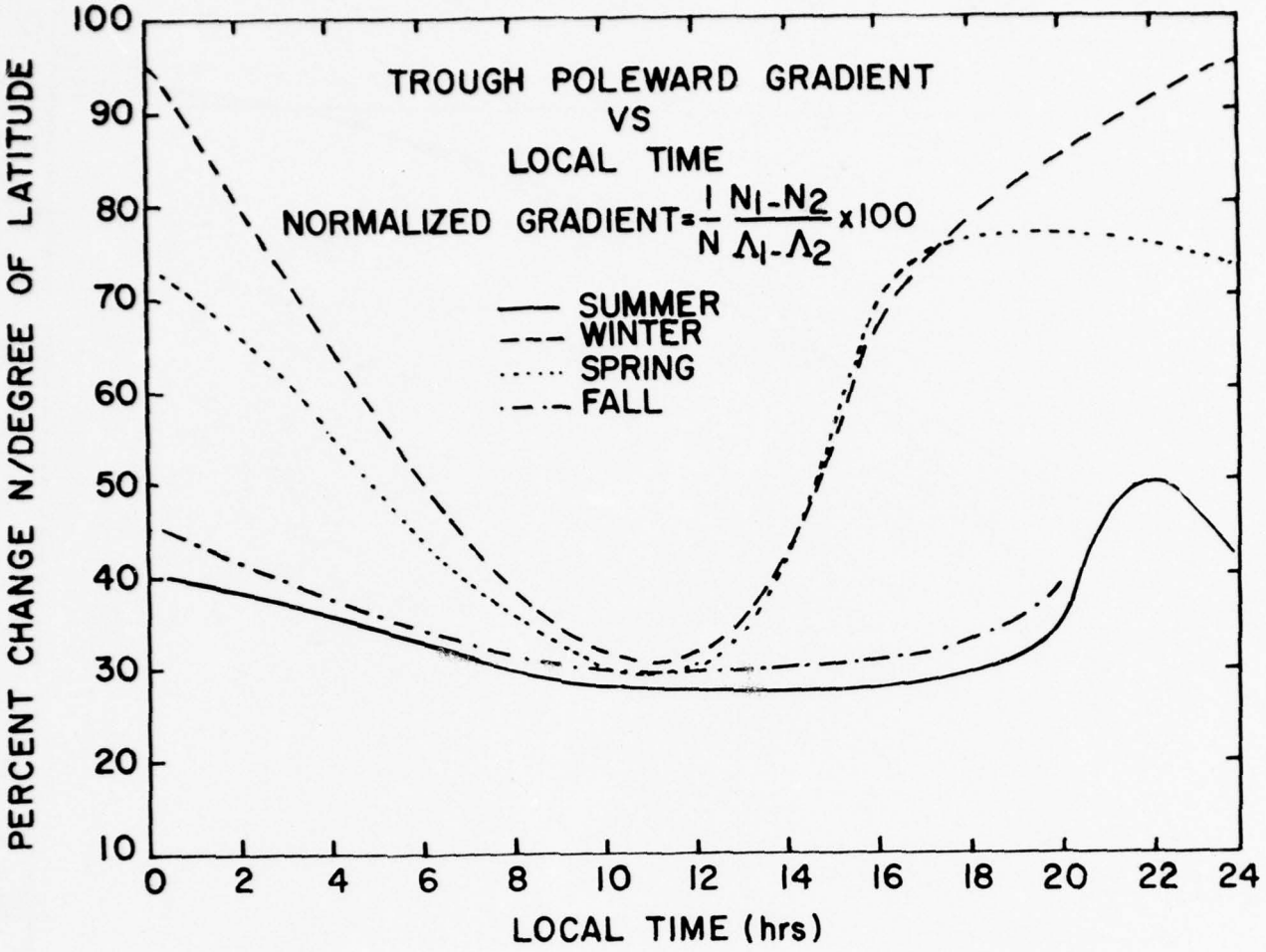

Figure 11. Normalized equatorial edge trough gradient vs local time

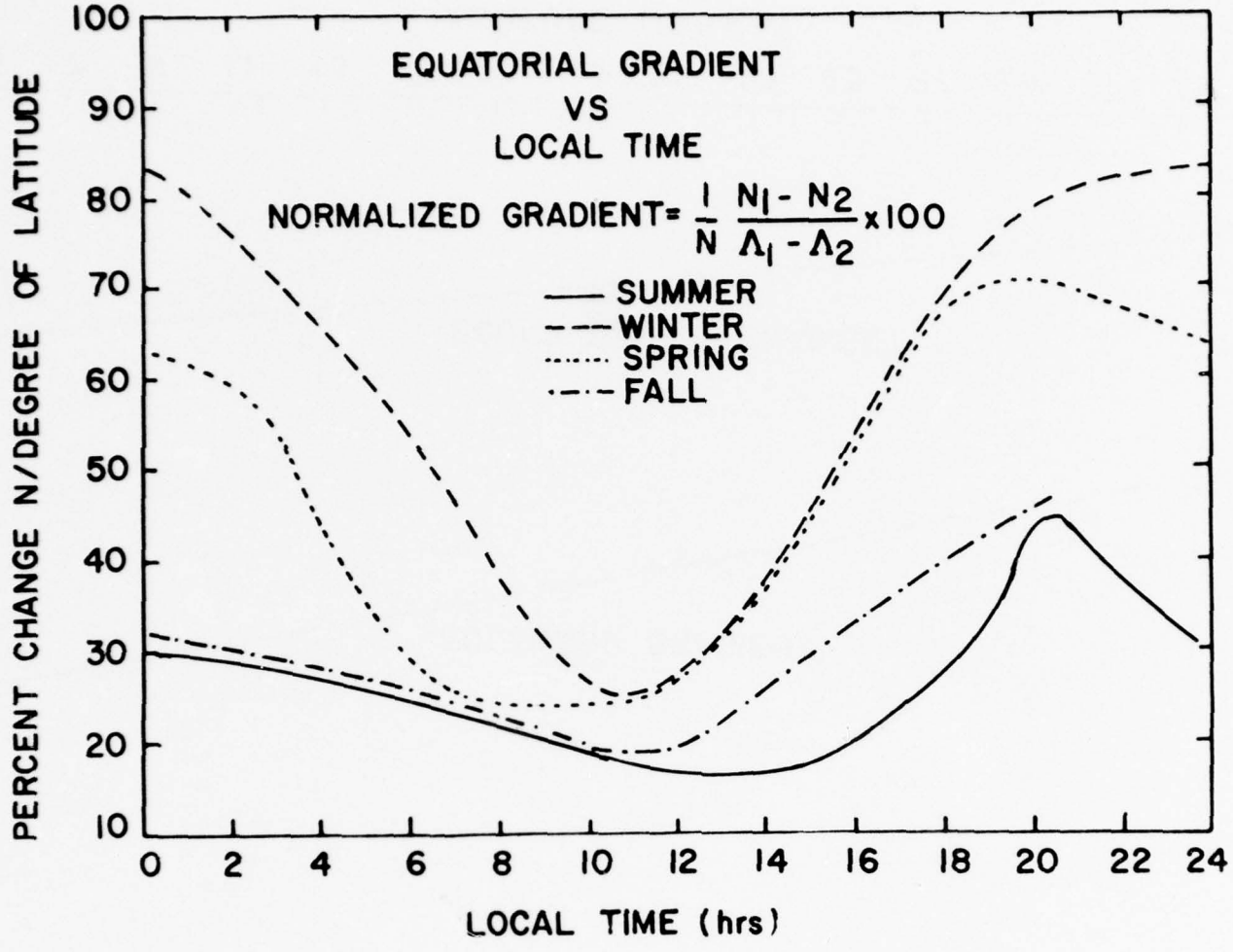

Figure 12. Normalized poleward edge trough gradient vs local time

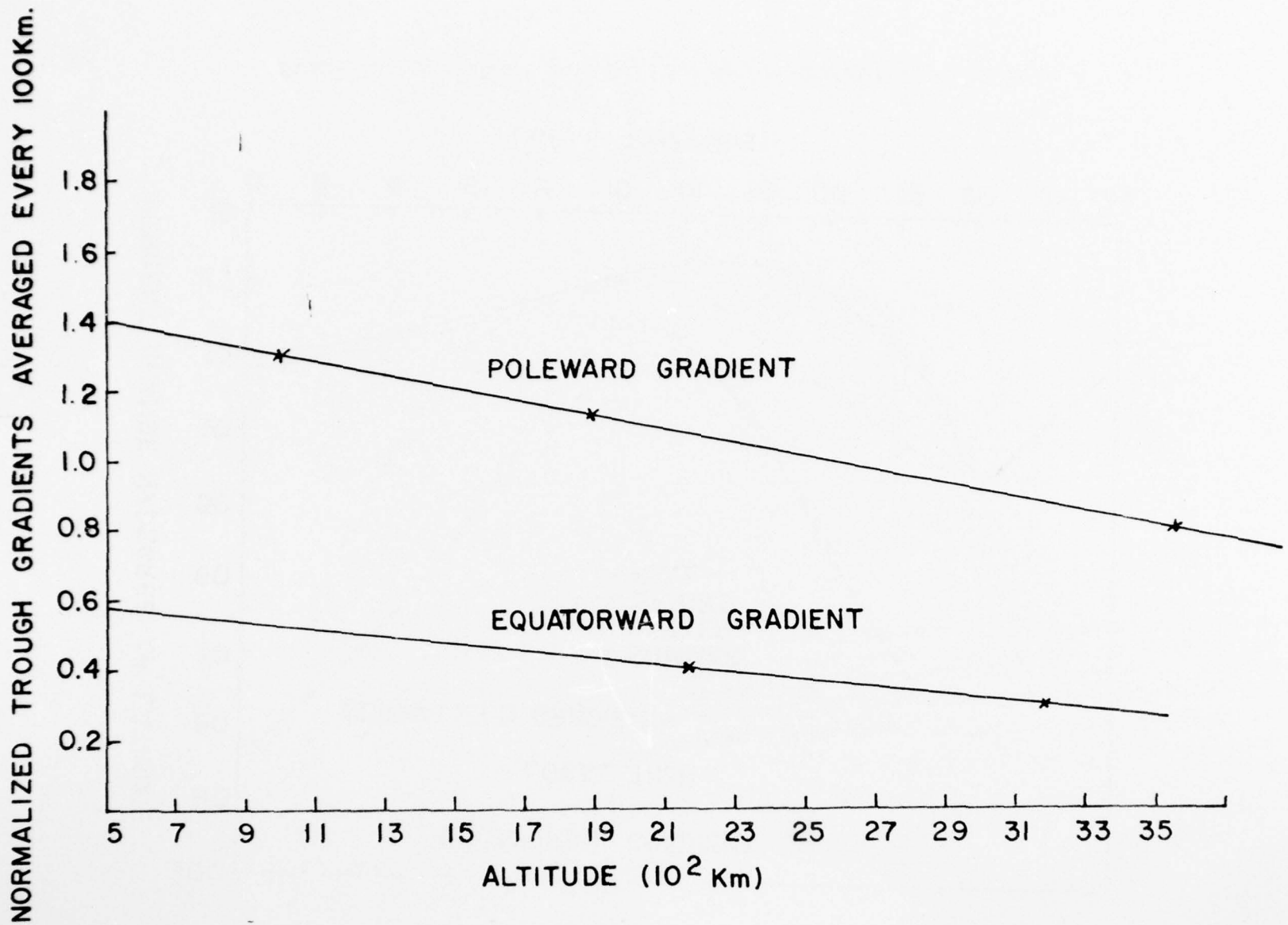

Figure 13. Equatorial and poleward gradient, lines of best fit

$0.62 - 9.82 \times 10^{-3} \times$ Alt. (1) Trough poleward gradient $(\frac{1}{N}\frac{dN}{d\Lambda}) =$ $1.44 \times 18 \times 10^{-3} \times$ Altitude (2) A comparison of the empirical equations (1) and (2) shows that the poleward gradient at a given altitude is about 2.5 times the equatorward gradient.

2.7 SOURCES OF VARIATION IN STATISTICAL RESULTS

An exhaustive investigation of the sources of variation in statistical results of the various trough parameters was made. It was found that using all data for $Kp \leq 3$ and treating them as representative of quiescent magnetic conditions is erroneous. This study revealed that under strictly controlled altitude conditions over a narrow local time sector, the trough parameters vary for Kp values from 0 to 3. Hence, our statistical values should be considered as the mean values over the Kp range 0 to 3. Furthermore, the usual practice of assignment of Kp values to trough measurements made at the same time is not strictly correct, as this procedure ignores the previous magnetic history of the ionosphere that could influence the measurements at a later time. It should also be borne in mind that the data analyzed in this report covered several seasons over the period of four years, and hence, could be influenced by the changing solar, magnetic, and ionospheric conditions and are bound to reflect some variations.

2.8 DISCUSSION OF RESULTS

In this report, we have presented only results for low Kp, ($Kp \leq 3_0$). We have carried out a similar analysis of a smaller sample high Kp data. The results on the trough structure are found to be surprisingly similar to the results at low Kp with the location moved to lower latitudes.

It is instructive to relate these results on the trough location to independent measurements of the plasmapause location from the same satel-

lite by Brace and Theis (1974), and by Miller (1974) as well as with other higher altitude measurements of the plasmapause.

Brace and Their reported gradients in electron density above 2000 km on the dayside from ISIS-I. They associate these gradients with the plasmapause location. We observe similar gradients with our own ion probe on ISIS-I on over 60% of the data near this location at altitudes above 2000 km. Figure 14, for example, gives results for the midday pass 6325. A low latitude density gradient is seen at about L = 3 together with a high latitude trough observed at 78° latitude. We consider that the low latitude gradients indicate the partial filling of flux tubes at low latitudes. The high latitude dayside trough would not normally be seen in the analysis carried out by Brace and Theis since they used a spatial resolution of about 9° in their analysis.

In Figure 15, we compare the equatorward edge of the trough with the plasmapause location observed by others. In addition the cross-hatched region on the dayside (between L = 2 and 4) indicates the location of low latitude high altitude density depressions mentioned above. It is seen that on the nightside, the trough location agrees with the plasmapause location reported by other workers. On the dayside, two regions of plasma depletion are observed. First, the high latitude trough observed at all altitudes located at the equatorward edge of the cusp. Second, plasma depletions between L = 2 and 4 at altitudes greater than 1500 km. Since they occur on lower L shells than the normal plasmapause, we consider that they represent partial filling of plasmasphere flux tubes as described by Banks and Doupnik (1974).

Finally, we must consider how these data add to our understanding of

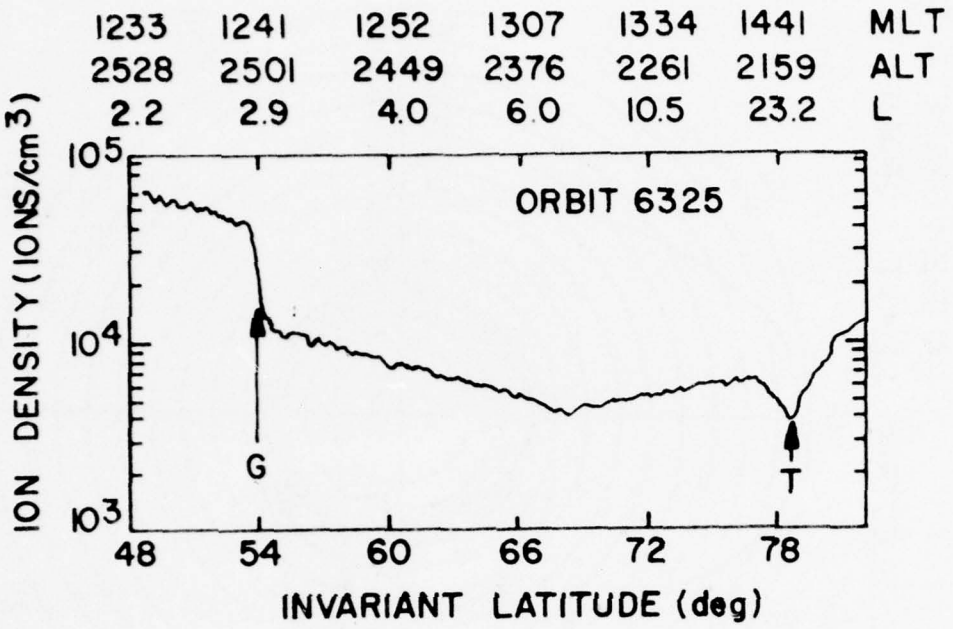

Figure 14. Ion density vs invariant latitude, orbit 6325

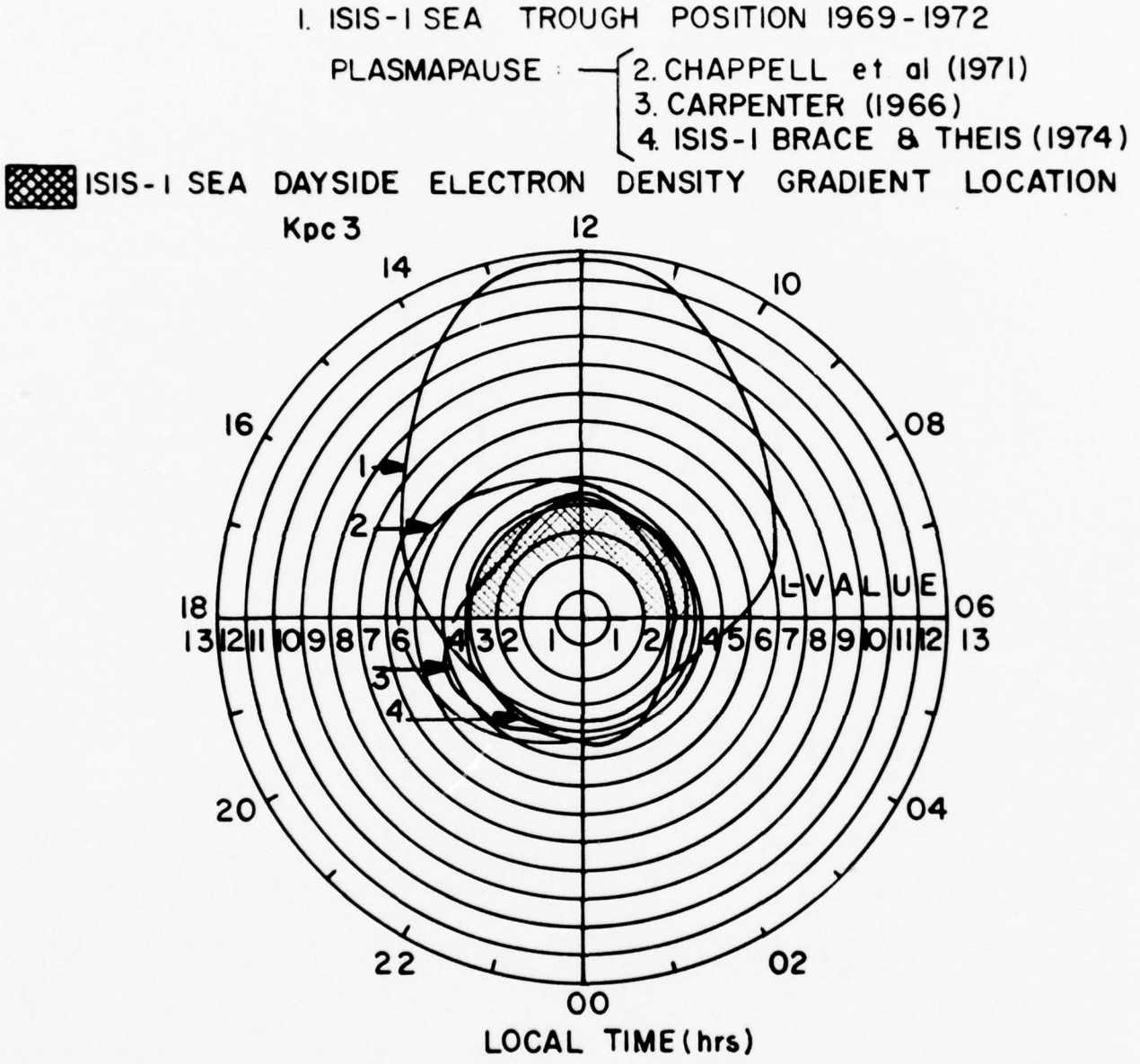

Figure 15. Comparison of trough position determined from the ISIS I SEA with plasmapause location determined from other sources and with the dayside electron density gradient location determined from the ISIS I SEA.

the formation of the trough. Since they are real data, gathered on a global scale over several years, we cannot dismiss them if they do not fit current theories of the formation and maintenance of the trough. In particular, the existence of daytime troughs means that solar UV cannot always be the major determining cause of trough formation. Since the daytime trough has a lower probability of occurrence and is less pronounced than at night, we must conclude that competing processes control the plasma density and motion at different times, and that these can sometimes overcome the constant replenishment of ionization by solar UV on the dayside. The most important of these is convective drift across the polar cap to supply plasma at night.

Other processes which influence the trough and its location include, on the nightside: 1. Auroral particle precipitation, causing ionization to give the poleward boundary; 2. The escape of light (H^+ and He^+) along open field lines to give depletion of plasma within the trough; 3. The presence of electric fields within the trough regions. This causes bulk motion of the plasma (direct depletion) in addition to Joule heating as this flow takes place. This heating increases the reaction rate of $O^+ + N_2 - NO^+ + N$, further reducing total ionization present above the F region peak.

The processes used by E fields become very important in the formation of the trough at latitudes and altitudes where H^+ is not the dominant ion, and where the more classical picture of ion escape along magnetic field lines is usually invoked as the major cause of ion depletion.

On the dayside, the poleward edge is again set by the particle precipitation. At the equatorward edge, however, the location shown in Figure 12 around L = 8 - 12 for several hours each side of local noon, fits more closely with the cusp location than with the plasmapause.

2.9 CONCLUSION

1. The trough is found to exist at all local times. It is not only a nighttime phenomenon. It is consistently found at the equatorial edge of the precipitation zone.

2. Significant variation of the widths, amplitude, and gradients at both the equatorial and poleward trough wall are found with local time and season. Maximum values are observed on winter nights.

2.10 REFERENCES

Banks, P. M. and J. R. Doupnik, Thermal proton flow in the plasmasphere: The morning sector, Planet. and Space Sci., 22, 79-94, 1974.

Brace, L. and R. F. Theis, The behavior of the plasmapause at mid-latitudes: ISIS-I Langmuir probe measurements, J. Geophys. Res., 79, 1871-1884, 1974.

Miller, N., The dayside mid-latitude plasma trough, J. Geophys. Res., 79, 3795-3801, 1974.

Tulunay, Y., and J. Sayers, Characteristics of the mid-latitude trough as determined by the electron density experiment on Ariel 3, J. Atmos. Terr. Phys., 33, 1737-1761, 1971.

3. SCINTILLATION STUDIES

Ionospheric Scintillation studies are being investigated in the high latitude and equatorial regions.

The original studies in the high and polar latitudes are being extended to investigate the local time, seasonal and geophysical variations. Features associated with scintillations in the low and equatorial regions are being identified, and their latitudinal extent, longitudinal dependence, seasonal and local time characteristics will be evaluated. Information on equatorial scintillations is very sparse and the Air Force is greatly interested in

this project.

The data for this investigation are the measurements of ion density made simultaneously by the ISIS-I SEA experiment and the RF Scintillation from the ATS 3 and 5 satellite recorded at the three ground stations: Narsarssuaq (Greenland), Hamilton (Massachusetts), and Huancayo (Peru).

4. AURORAL OVAL STUDIES

A preliminary study was made to investigate the feasibility of using the 'Q' Auroral index as a measure of polar cap size and activity. Comparative studies have been made with results from simultaneous experiments. The results are not entirely satisfactory. However, it is felt that more work has to be done in this regard to get a conclusive picture. Satellite and other supporting data recorded during the extensively studied magnetic storm of December 1971 was suggested for this study.

5. THE DECEMBER 1971 MAGNETIC STORM STUDY

The importance of this magnetic storm for a comparative study with other simultaneously collected ionospheric data was discussed at the April 8-9, 1975 AFCRL-Air Weather Command meeting held at AFCRL. It was suggested that an extensive investigation be made of this period using ISIS-I data to obtain values of the different characteristics of the trough and of the precipitation regions.

6. TOPSIDE STRUCTURE MONITOR

The Defense Meteorological Satellite Program (DMSP) office at SAMSO and the Air Weather Service (AWS) and the Global Weather Central (GWC) have planned the launch of Topside Ionosphere Structure Monitors beginning in the latter part of 1977.

Electron and ion sensors on the Topside Ionosphere Structure Monitor

will measure in situ ion and electron density and temperature and the scale height (H) in the topside ionosphere. These plasma measurements will provide inputs to AWS and GWC ionospheric prediction programs for the determination of total electron content and electron density profiles. The plasma irregularity meaurements can identify the mid-latitude electron trough which will be used to determine whether low, mid, or high latitude prediction programs should be used to provide propagation conditions to operating commands. The satellite data from these instruments when properly analyzed and interpreted will extend the capability of the Air Force to provide global information on several ionospheric parameters of importance to communications, surveillance, and detection systems.

The single in situ measurements of plasma parameters along the orbital path of about 800 km are to be used in monitoring the critical frequency of the F_2 (f_0F_2) layer and the scale height (H) near the F_2 peak. This type of information is very sparse over less populated and oceanic areas and hence, this DMSP program will fill this need.

Further investigations of the various models of the ionosphere were made. Mechanisms for the calculation of H (the scale height) in the nose region of the parabolic ionization are being investigated with a view to developing theoretical models. Our studies show that the exponential model fits the ionization variation well up to an altitude of nearly 800 km. The Damon model gives unsatisfactory results.

The accuracy of the models depends upon the values of the M factor obtained from ITSA data books. The magnitude of errors introduced in the f_0F_2 values due to the sparse coverage of M values in certain latitude and longitude regions have been evaluated. To investigate the structure of

the ionosphere in the region 300-1000 km, models of the atmosphere have to be developed by incorporating the variations in temperature, density and scale height near the peak of the F_2 region. Preliminary studies have already been made and are supplemented by incorporating new material from the back scatter radar measurements by J. V. Evans at Milestone Hill, Massachusetts. Some additional work has been done on the nature of temperature variation with altitude in the region above the F_2 peak. This will be used in the development of empirical models of the topside ionosphere. Computations of the scale height (H) above the F_2 peak were made using averaged values of mean ionic masses and plasma temperatures for the day and night times. These calculations give information about the magnitude and direction of the scale height variation.

Theoretical models of distribution of ionization in the topside, like the Damon model and the exponential (Bent) model have been examined using measured values of electron density profiles from the ISIS-I topside ionograms, kindly provided us by Dr. Whitteker of Canadian Department of Communications, Ottawa, Canada.

Mapping of irregulatities in the topside ionosphere down to the F_2 peak was critically investigated. This showed that irregularities do not map along field lines but they can be recognized easily for a change of altitude at any given geographic latitude and longitude.

7. PRESENTATIONS AND PUBLICATIONS

1. Sagalyn, R. C., P. J. L. Wildman, and M. Ahmed, Structure and Morphology of the Main Trough in the Topside Ionosphere, AFGL Scintillation Review, February 1976.

2. Wildman, P. J. L., R. C. Sagalyn, and M. Ahmed, Structure and

Morphology of the Main Plasma Trough in the Topside Ionosphere, EOS, April 1976.

3. Wildman, P. J. L., R. C. Sagalyn, and M. Ahmed, Structure and Morphology of the Main Plasma Trough in the Topside Ionosphere, Proc. COSPAR Symposium on the Use of Satellite Beacon Observations, Boston, June 1976.

4. Sagalyn, R. C., P. J. L. Wildman, and M. Ahmed, Plasma Boundaries at Mid and High Latitudes in the Topside Ionosphere, ISIS-I Working Group Meeting, Boulder, June 1976.

8. FIGURES CITED IN THE TEXT

DEVELOPMENT, CALIBRATION AND INTEGRATION OF ELECTRICAL AND MECHANICAL INSTRUMENTATION FOR SCIENTIFIC EXPERIMENTS

PETER B. ANDERSON

1. INTRODUCTION

This section describes the engineering activities during this contract period. Individual project areas have been subdivided for clarity.

2. AEOLUS ROCKETS

Develop, calibrate, and integrate electrical and mechanical instrumentation for scientific experiments to be flown on two AEOLUS Rocket payloads.

(a) Electric Field and Electron Density Measurements (A10.302.1)

The objective of this experiment was to determine the electric field influence on ion and electron motion. This was accomplished by launch- three rockets, the first two of which were chemical cloud releases followed by a third carrying the diagnostic instrumentation through the chemical cloud. The instruments for measuring the electric fields and electron densities were designed under this contract. The flight instrumentation consisted of four motorized electric field antennae, electron density sensor/ boom assembly, electron density LOG electrometer, and a main electronics package. The interconnection diagram showing the above units is shown in Figure 1.

The engineering effort for the above instrumentation included circuit design, printed circuit layouts and electron density sensor, and electronics package design. The electron density system consisted of a LOG electrometer and level shifter module. Within the electronics package were several printed circuit board assemblies. Each printed circuit (PC) board performed specific system functions. Board level functions include the power supply program timer, sweep/calibration, program monitor, difference amplifiers, and electrometers. A schematic of the four electric field electrometers is shown in Figure 2. After the flight hardware was fabricated by AFGL, the instruments were aged with temperature. Next, the flight system was calibrated in all modes of operation. Finally, travel to NRC at Churchill,

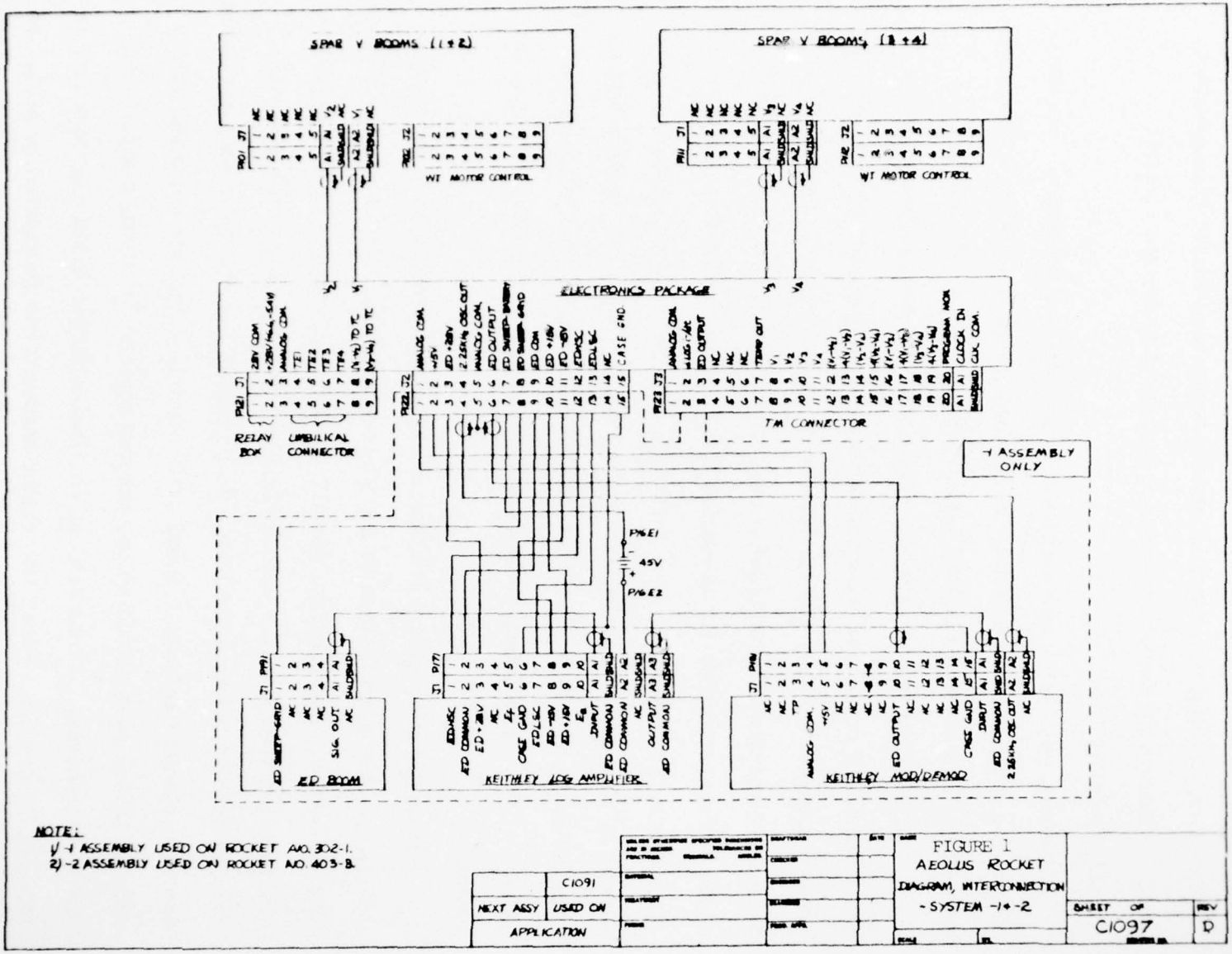

NOTE:
1) -1 ASSEMBLY USED ON ROCKET A/O 302-1.
2) -2 ASSEMBLY USED ON ROCKET A/O 403-B.

	C1091
NEXT ASSY	USED ON
APPLICATION	

FIGURE 1
AEOLUS ROCKET
DIAGRAM, INTERCONNECTION
- SYSTEM -1 & -2

SHEET OF C1097 REV D

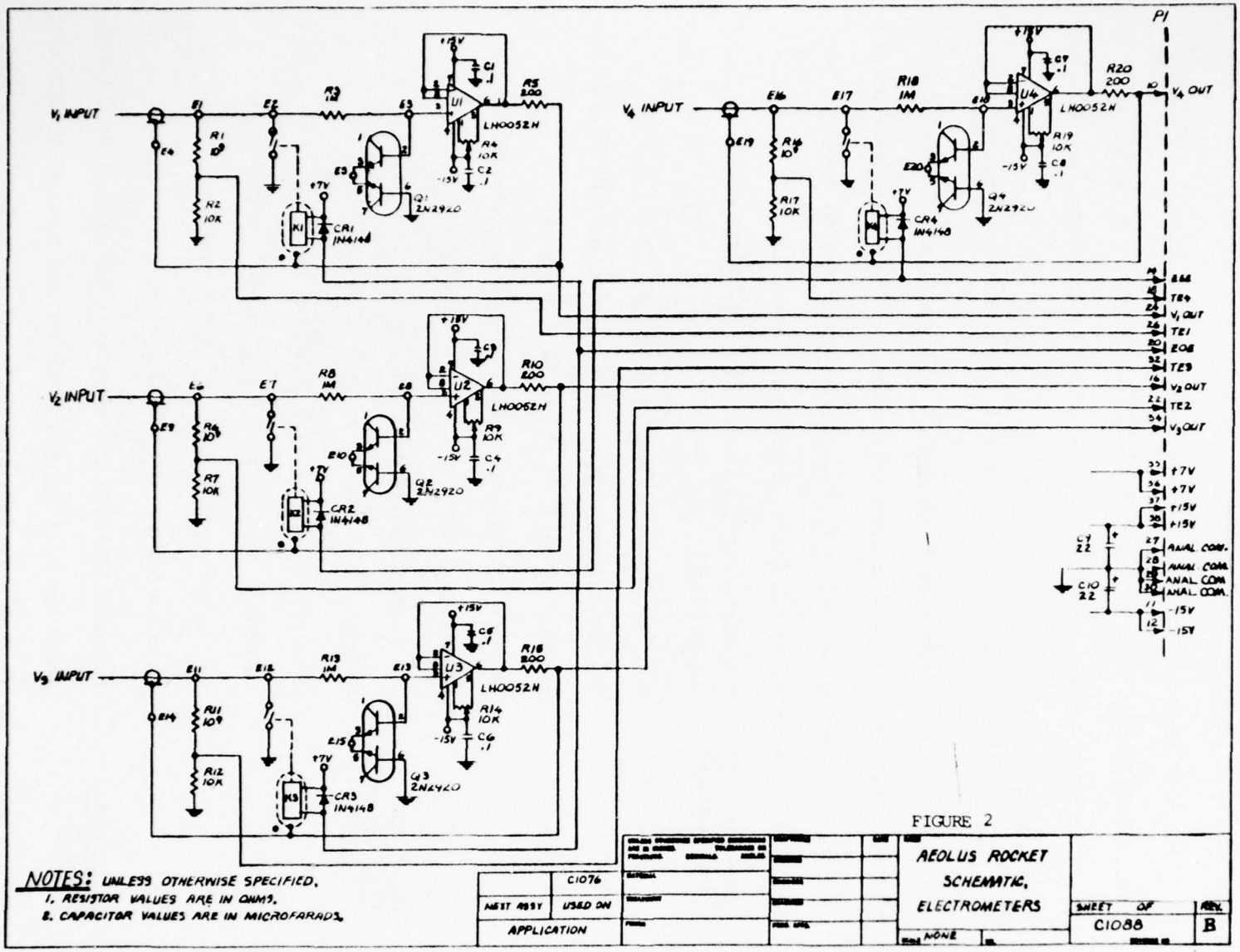
P1
V1 INPUT
V2 INPUT
V3 INPUT
V4 INPUT
LH0052H
2N2920
IN4148
+15V
-15V
+7V
ANAL COM.
V1 OUT
V2 OUT
V3 OUT
V4 OUT
NOTES: UNLESS OTHERWISE SPECIFIED,
1. RESISTOR VALUES ARE IN OHMS.
2. CAPACITOR VALUES ARE IN MICROFARADS.
C1076
NEXT ASSY
USED ON
APPLICATION
AEOLUS ROCKET
SCHEMATIC,
ELECTROMETERS
SHEET OF
C1088
REV.
B

FIGURE 2

Manitoba, Canada, was made in support of the launches.

(b) Electric Field Measurements (A10.403.3)

For this payload, instrumentation was required for only the electric field measurements. The electric field flight system was identical to the above hardware and was prepared in parallel with it. Launch was made at a later date, but on the same field trip to NRC.

3. DMSP SATELLITE (SSI/E)

Ionospheric plasmas monitors (SSI/E) will be flown on three (3) Block 5D DMSP satellites to make in-situ measurements of topside plasma scale height, small-scale ionization irregularities and F region critical frequencies. The SSI/E system design consists of the following:

Electron Probe: (Boom Mounted)
A spherical electrostatic analyzer (2¼" dia.)
Weight: 0.16 lbs.
Density range: 10 to 5 x 10^5 per cm^3
Corresponding F region critical frequencies 1 to 30 mHz
Current range: -10^{-5} to -10^{-10} amperes
Temperature range: 1000 to 15,000 degrees Kelvin
Satellite potential: +5 to -10 volts

Ion Probe: (Boom Mounted)
A planar electrostatic analyzer (3" dia. x 1.9")
Weight: 0.62 lbs.
Density range: 10 to 5 x 10^5 per cm^3
Current range: 5 x 10^{-7} to 5 x 10^{-12} amperes
Temperature range: 1000 to 15,000 degrees Kelvin
Ion mass range: 1 to 35 amu

Electronics Package:
Includes positive and negative electrometer amplifiers, sweep and bias circuits, timing and control electronics, digital interface circuitry and power converter. Dim.: 4"x4"x6"
Weight: 2.92 lbs.

System Specifications:

Total Weight - 3.7 lbs. (Excluding Booms and S/C Harness)

Total Power - 3.0 watts

Total Volume - 150 in^3 (Excluding booms)

Telemetry - 180 bits per second

Six samples per second are taken on each of 2 sensors resulting in a spatial resolution of 1.0 km for the electron density measurement. A plasma temperature measurement is made every 900 km.

Considerable time went into developing low power LOG electrometers for measuring positive and negative current over a five (5) decade range with a minimum current of 10^{-12} amperes. The outputs of the electrometers change at a rate of 1 volt per decade of input current. A schematic of SSI/E electrometers is shown in Figure 3. The electron probe is connected to the negative LOG electrometer and the ion probe is connected to the positive LOG electrometer. The electrometers are located on a printed circuit board within the electronics package. The electronics package also contains the rest of the system circuits which are separated from the electrometers by a shield. Other printed circuit board designs contain the level shifter circuits and analog telemetry monitors, sweep and calibration control circuits, program timer, and digital data interface circuit. Since the electrometers and their outputs are floating at potentials with respect to circuit common, level shifter circuits are required to reference the electrometer outputs to telemetry common. The level shifting is accomplished by a differential amplifier which measures the difference between the electrometer common and the electrometer output. The output of each level shifter circuit is wired to the digital data interface board. The program timer circuit is clocked by a synchronized 1 H_z pulse (read pulse-SSI/ERED) from the spacecraft which is used for generating a 1024 sec program cycle. The

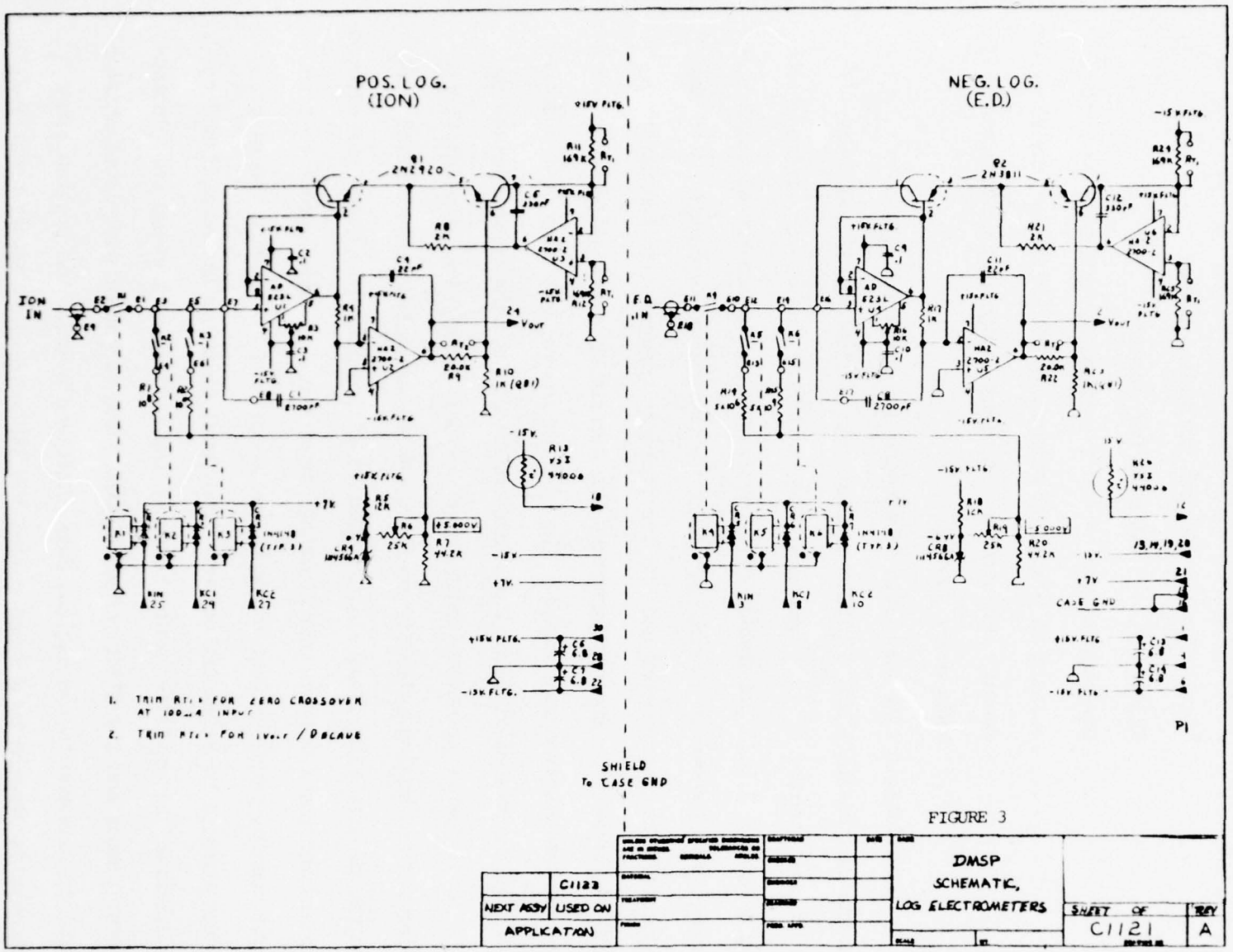

FIGURE 3

	C1123		DMSP SCHEMATIC, LOG ELECTROMETERS	SHEET OF C1121	REV A
NEXT ASSY	USED ON				
APPLICATION					

sequence of events within the program cycle is shown in Table 1.

Telemetry output consists of two analog lines and one digital line. The two analog lines monitor temperature and the resting bias mode which is programmable with a digital command signal. The digital line is a multiplexed signal which contains the electron, ion, and event monitor data. The digital data interface board converts the electron, ion, and event monitor analog signals into a single digital NRZ (non-return to zero) data signal, designated as (SSI/EDAT) to the OLS (Operational Linescan System). This data signal is transferred in phase with the OLS supplied bit clock in bursts of 180 contiguous bits at a bit rate of 1000 Hz $\pm$ 1 Hz. Upon command (SSI/ERED) from the OLS, the SSI/E provides one 180-bit data block per second with the least significant bit (LSB) occurring first in the first word.

The SSI/E 180-bit data block consists of twenty 9-bit data words as follows:

7 Samples Electron Data (Words 1, 4, 7, 10, 13, 16, 19)

7 Samples Ion Data (Words 2, 5, 8, 11, 14, 17, 20)

6 Samples Event Monitor (Words 3, 6, 9, 12, 15, 18)

All data is stored in SSI/E shift registers. Once per second a read pulse (SSI/ERED) of 180 ms duration from the OLS allows the registers to shift out data acquire during the 1000 ms period prior to the END of the read period as shown in Figure 4. Word 1 is shifted out first.

The above SSI/E circuit designs were initially breadboarded by AFGL and then evaluated for 6 months without experiencing a failure. After the breadboard evaluation, the flight printed circuit board designs were completed. Next, the flight sensors, printed circuit board assemblies, electronics package, and DC-DC converter assemblies were fabricated by AFGL. The following chart shows the status of the three flight systems on 30 April 1977.

Table 1. DMSP SSI/E Sequence of Events.

EVENT	APPLIED SIGNAL	EVENT MON LEVEL	DURATION (SEC)	TIME (SEC)	
				FIRST	REPEATS EVERY
CAL. NO. 1	$+5 \times 10^{-8}$ a (ION) -1×10^{-6} a (ELEC)	0.2V	2	0-2	1024
CAL. NO. 2	$+5 \times 10^{-11}$ a (ION) -1×10^{-9} a (ELEC)	0.4V	2	2-4	1024
ELECTRON SWEEP FLAG	NONE	0.6V	2	8-10	128
ELECTRON SWEEP (OUTER GRID)	+5V→ -8V	+5V → +1V	10	10-20	128
ION SWEEP FLAG	NONE	0.8V	2	24-26	128
ION SWEEP (OUTER GRID)	-5V - +12V	+1V - +5V	12	26-38	128

MODE	RESTING BIAS ELECTRON DENSITY GRID	MODE MON. LEVEL
1	1.5V	3.5V
2	0 V	1.5V

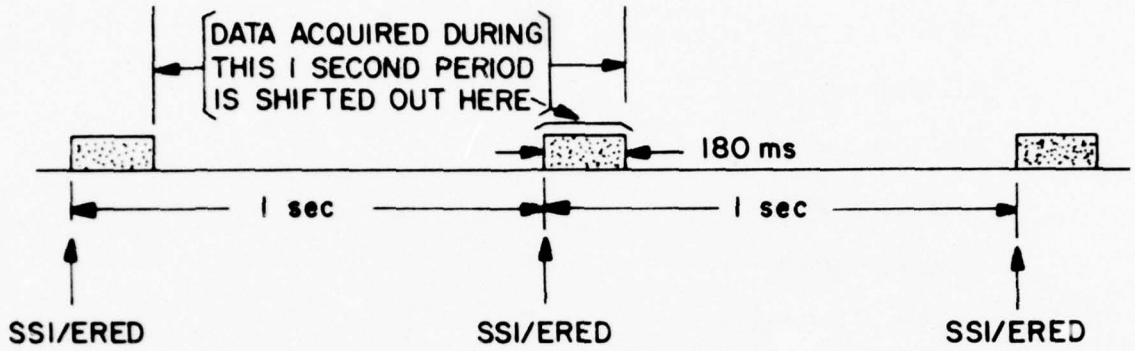

Figure 4. DMSP SSI/E data cycle.

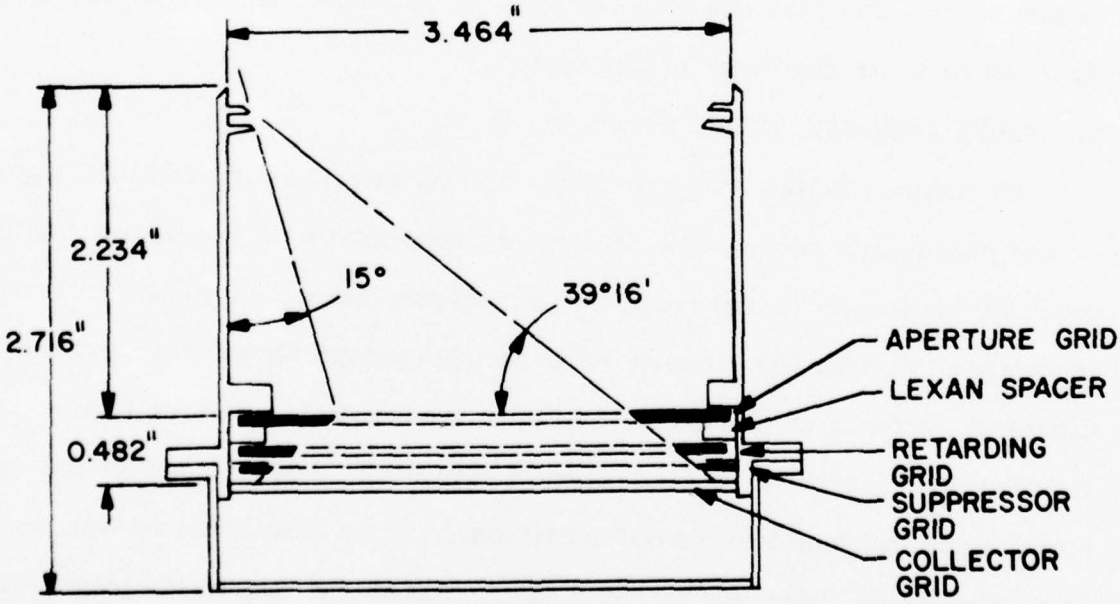

Figure 5. SCATHA surface and boom mounted instruments.

Function	S/N 1	S/N 2	S/N 3
Assembled	x	x	x
Aged	x	x	
Calibration	x	x	
RCA Integration	x		
Vibration Tests	x		
Thermal Vacuum	x		
Vandenberg GO-No GO	x		
Launched			

Travel to several sites in support of the first (S/N 1) SSI/E system was made. One trip to the Westinghouse plant was made to evaluate the digital interface between the satellite and the SSI/E digital data interface circuit. Also, several trips were made to RCA for the integration, vibration and thermal vacuum tests. Finally, one trip was made to Vandenberg AFB for a prelaunch Go-No Go test for the first flight system.

4. SCATHA SATELLITE (SC6-1, 2, and 3)

The Thermal Plasma Analyzer (SC6) will measure the direction and magnitude of the plasma bulk motion, the density and temperature of the plasma 'bath' in which the satellite is immersed, and investigate spacecraft-plasma interaction mechanisms by measuring fluctuation in vehicle potential and charging and discharge currents to the satellite due to environmental factors such as solar illumination, satellite motion, plasma temperature, density, and motion variations during quiet and disturbed conditions. It is also aimed at studies of these properties under controlled conditions when the spacecraft potential is varied by means of an electron gun. These constitute some of the prime measurements required to understand and solve the problem of spacecraft charging at high altitudes.

The Thermal Plasma Analyzer consists of three gridded sensors and an electronics package (SC6-3). Two sensors (SC6-1) are mounted on a boom 3 meters from the nearest space vehicle body-mounted components. The third sensor (SC6-2) is body-mounted on the conducting end of the space vehicle. The normal to the aperture of one boom sensor is parallel to the normal to the aperture of the surface sensor and also parallel to the space vehicle spin momentum vector. The second boom sensor normal is perpendicular to the spin vector. The experiment will measure, by retarding potential analysis, the environmental electron and ion densities in the range 10^{-1} to 10^{4} per cm^{3} and particle energies in the range 0.1 to 100 eV.

Basic mechanical design of the gridded probe is shown in Figure 5. The combined measurements from the surface mounted sensor and the boom mounted units make it possible to ascertain the influence of photoelectrons from the spacecraft surface. Photoelectron production within the sensor is further minimized by restricting the sensor aperture field of view to a 15^{o} half-angle cone. Depending on the voltage of the collector and stepped grid, electrons or positive ions will be measured. During disturbed conditions the vehicle potential may exceed 100 V negative. In this case, the potential is determined from the positive ion sensor where the thermal ions arrive at the vehicle with average energies equal to their thermal energy plus that imparted by the energy equivalent of the spacecraft potential.

The electrical configuration of the sensors is shown in Figure 6. Using ground commands A, B, and C, the boom and surface mounted sensors can be operated in a large number of ion or electron modes. Commands D, E, F, and G select eight (8) aperture-bias levels ranging from -50 V to +50 V.

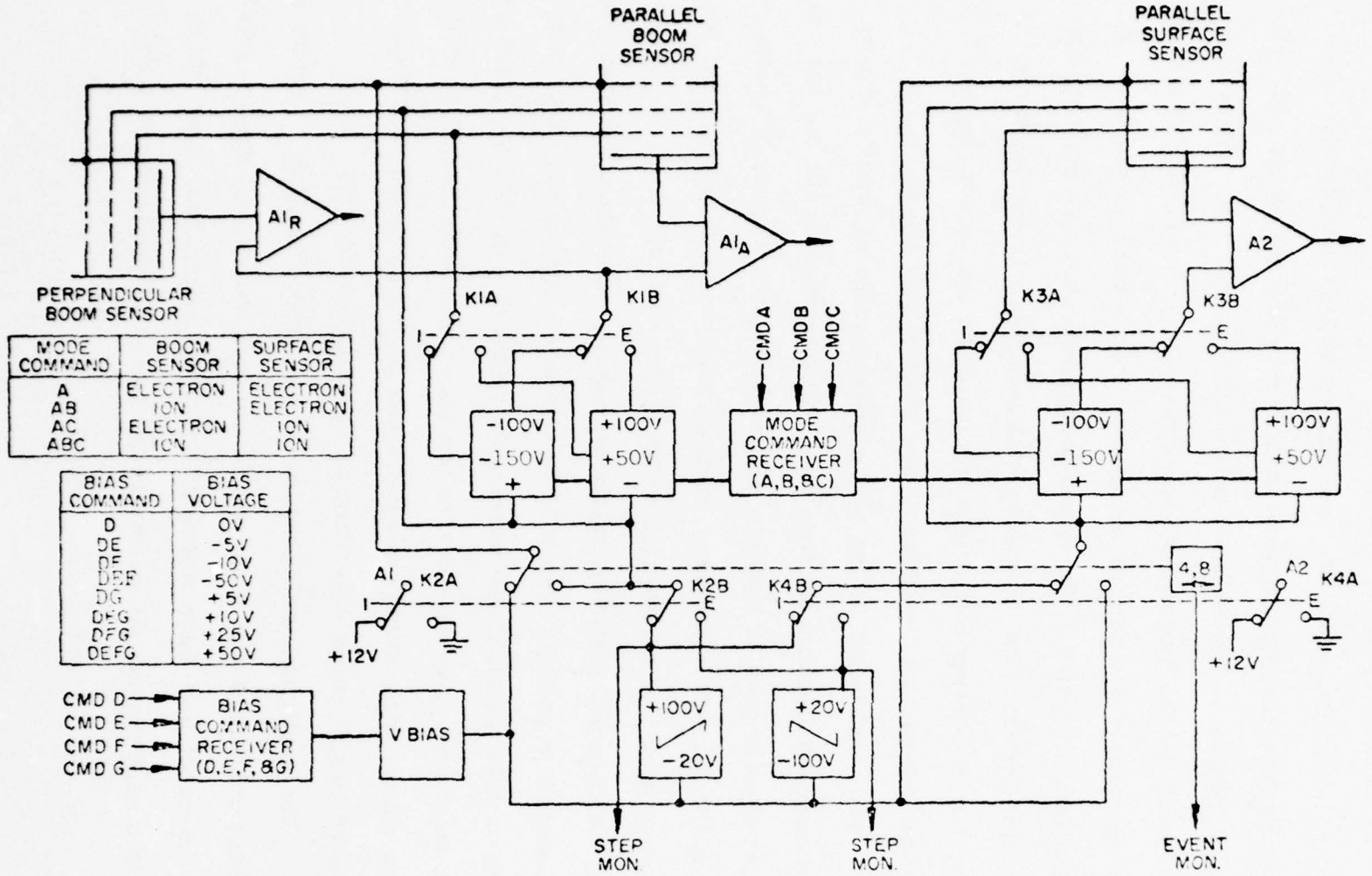

MODE COMMAND	BOOM SENSOR	SURFACE SENSOR
A	ELECTRON	ELECTRON
AB	ION	ELECTRON
AC	ELECTRON	ION
ABC	ION	ION

BIAS COMMAND	BIAS VOLTAGE
D	0V
DE	-5V
DF	-10V
DEF	-50V
DG	+5V
DEG	+10V
DFG	+25V
DEFG	+50V

Figure 6. SCATHA sensor electrical configuration.

4.1 SC6-3 ELECTRONIC CIRCUIT DESCRIPTIONS

The system Block Diagram (Figure 7) shows the major experiment components in addition to specific circuits developed for the main electronics package SC6-3. The following paragraphs provide a brief description of these circuits and their relationship to one another.

4.2 ELECTROMETERS

The linear range switching electrometers (Figure 8) are current to voltage amplifiers designed to have an output of 0 to 5 V for each decade of input current. Each sensor's electrometer is programmed to measure either ions or electrons. The electrometer uses a MOSFET operational amplifier at the input to measure four decades of current over the range 10^{-13} to 10^{-9} A. As the output voltage approaches 0 or 5 V, the electrometer is automatically switched into the next current range. Internal calibration signals are applied to the electrometer input in each range approximately once every hour.

Because extremely high values of feedback resistors (R_F) are necessary, the electrometer circuits tend to be temperature dependent. Therefore, a separate temperature monitor (thermistor) is provided for each electrometer. These outputs will be used to determine in-flight amplifier characteristics based on preflight laboratory temperature calibrations and testing.

To achieve the various operation modes of the experiment, several fixed and varying voltage signals must be periodically applied to the electrometer common and sensor elements. To do this, the electrometer common must be electrically floating with respect to the system common or spacecraft ground. Since the electrometer output voltage is consequently "riding on" the varying signals being applied to the electrometer common, a level shifter circuit must be employed to reference the 0-5 V output signal to system common.

4.3 LEVEL SHIFTERS

Each level shifter circuit is a differential operational amplifier which

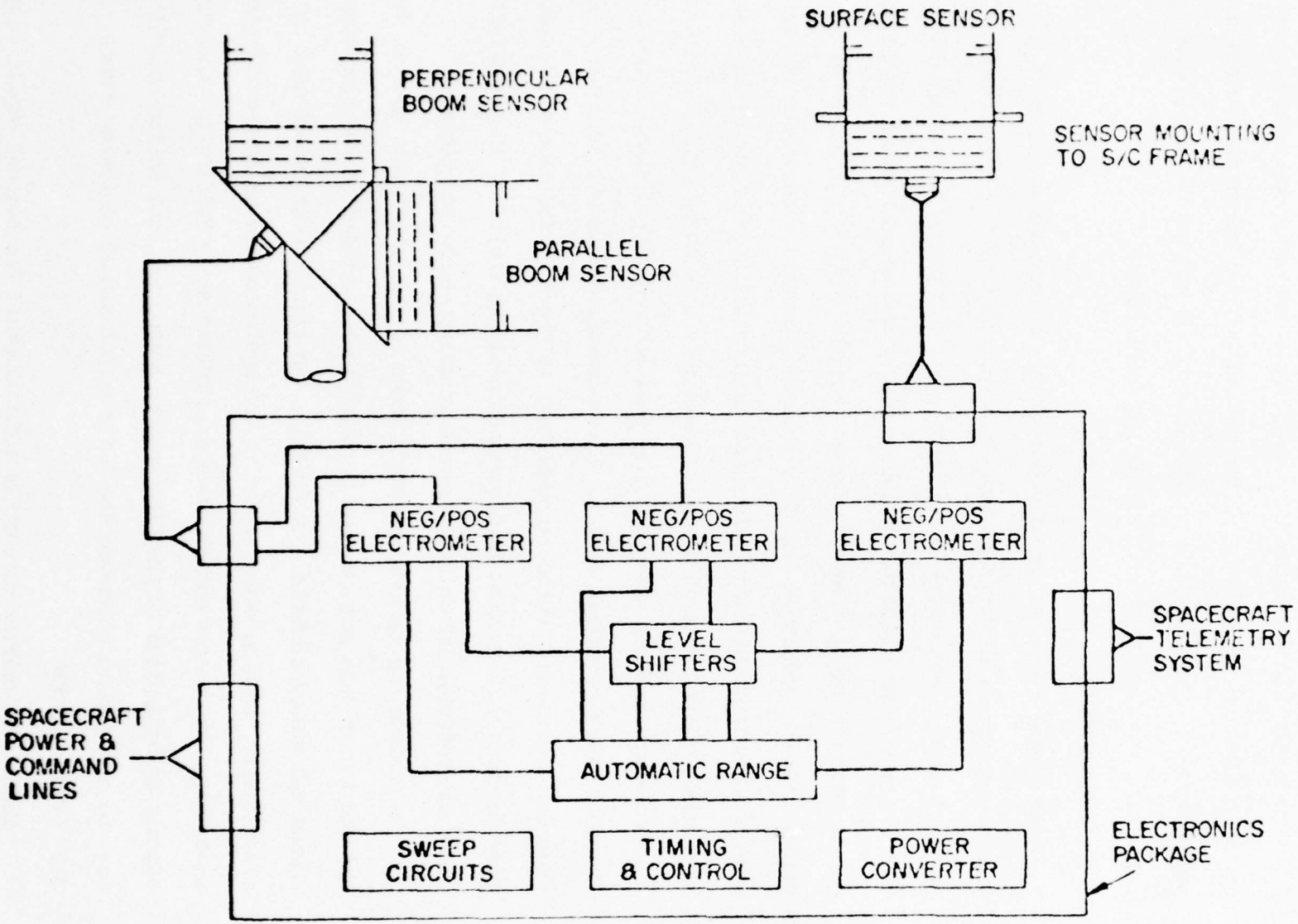

Figure 7. SCATHA SC6 thermal electron/ion measurement experiment.

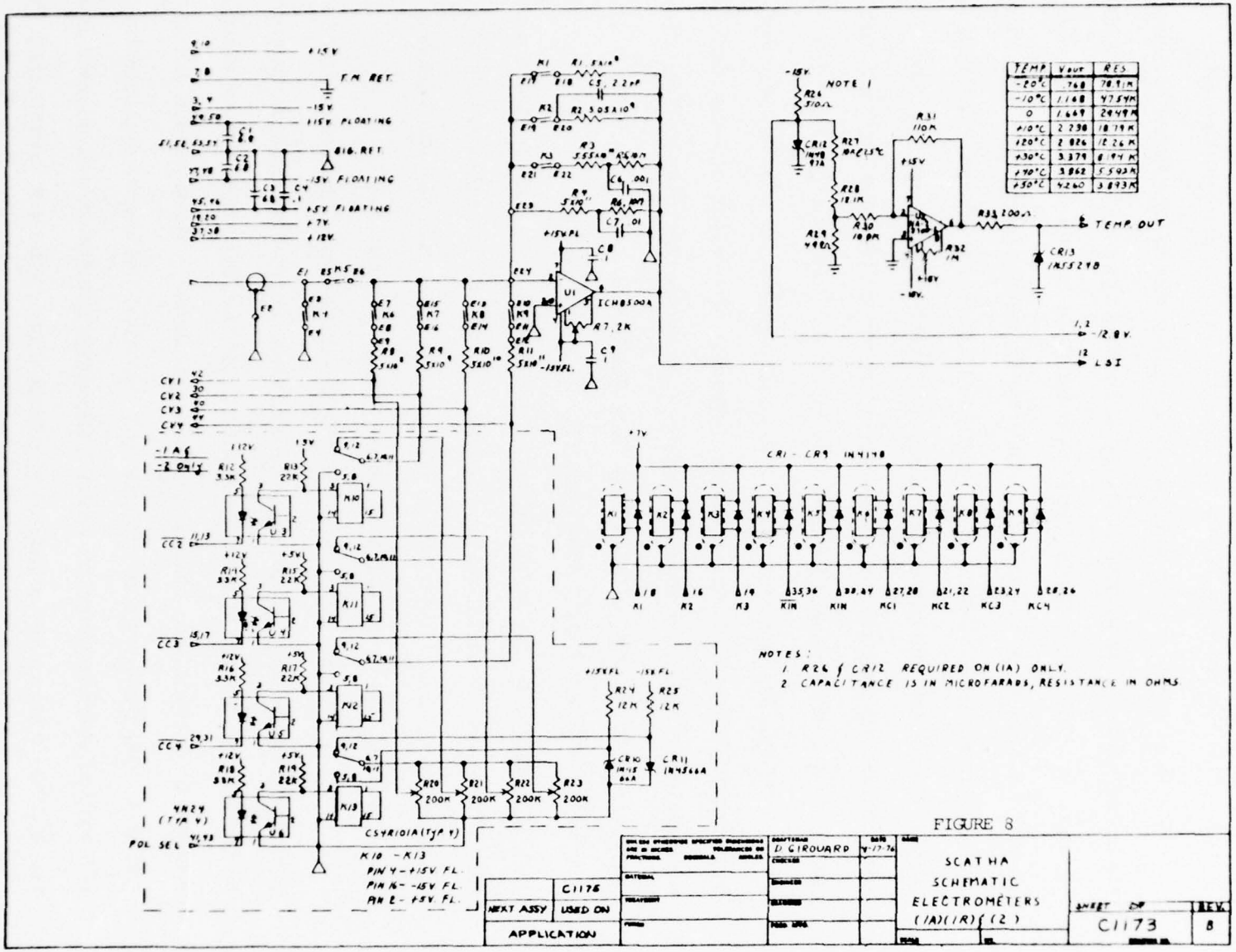

TEMP	V OUT	RES
-20°C	.768	78.7K
-10°C	1.168	47.5K
0	1.669	29.49K
+10°C	2.238	18.79K
+20°C	2.826	12.26K
+30°C	3.379	8.19K
+40°C	3.862	5.593K
+50°C	4.260	3.893K

FIGURE 8

measures the difference between the electrometer common and the electrometer output. The electrometer common is floating with respect to telemetry common.

The level shifting is achieved by dividing the electrometer common and the electrometer output separately by 10, using the resistor divider networks as shown in Figure 9. Since the bias potentials on the electrometer may be as high as 120 V, this division is necessary to reduce these levels to within the maximum operating range of the operational amplifiers. The reduced output levels are then impedance matched through the voltage follower circuits U_1 and U_2 and applied to the input of the differential operational amplifier U_3, which amplifies the difference of the two signals by 10. Located between U_1, U_2, and U_3 is a switching arrangement to adjust for polarity differences between ion and electron signals. The output of U_3, which is referenced to circuit common, is sent to the spacecraft data transmittal system and to the automatic range-switching circuit.

4.4 AUTOMATIC RANGE-SWITCHING CIRCUITS

The output of the level shifter is connected to a comparator circuit which commands the range-switch circuit (Figure 10) to either step the electrometer up or down into a new sensitivity range. This happens whenever the level shifter output signal goes below 350 mV or above 5.0 V.

The up/down command line has a 400 msec delay network to filter out noise. After a positive command has been established, an up/down counter is advanced by one count. The counter has a Binary Coded Decimal (BCD) output which is decoded to operate reed relays in the electrometer. These relays are in the resistor feed-back loop and control the current to voltage relationship. The BCD outputs are also used to control the range monitor output voltage levels. The up/down counter is periodically jammed with a code for controlling the calibration of the electrometer. During this mode, the range-switch circuit is inhibited.

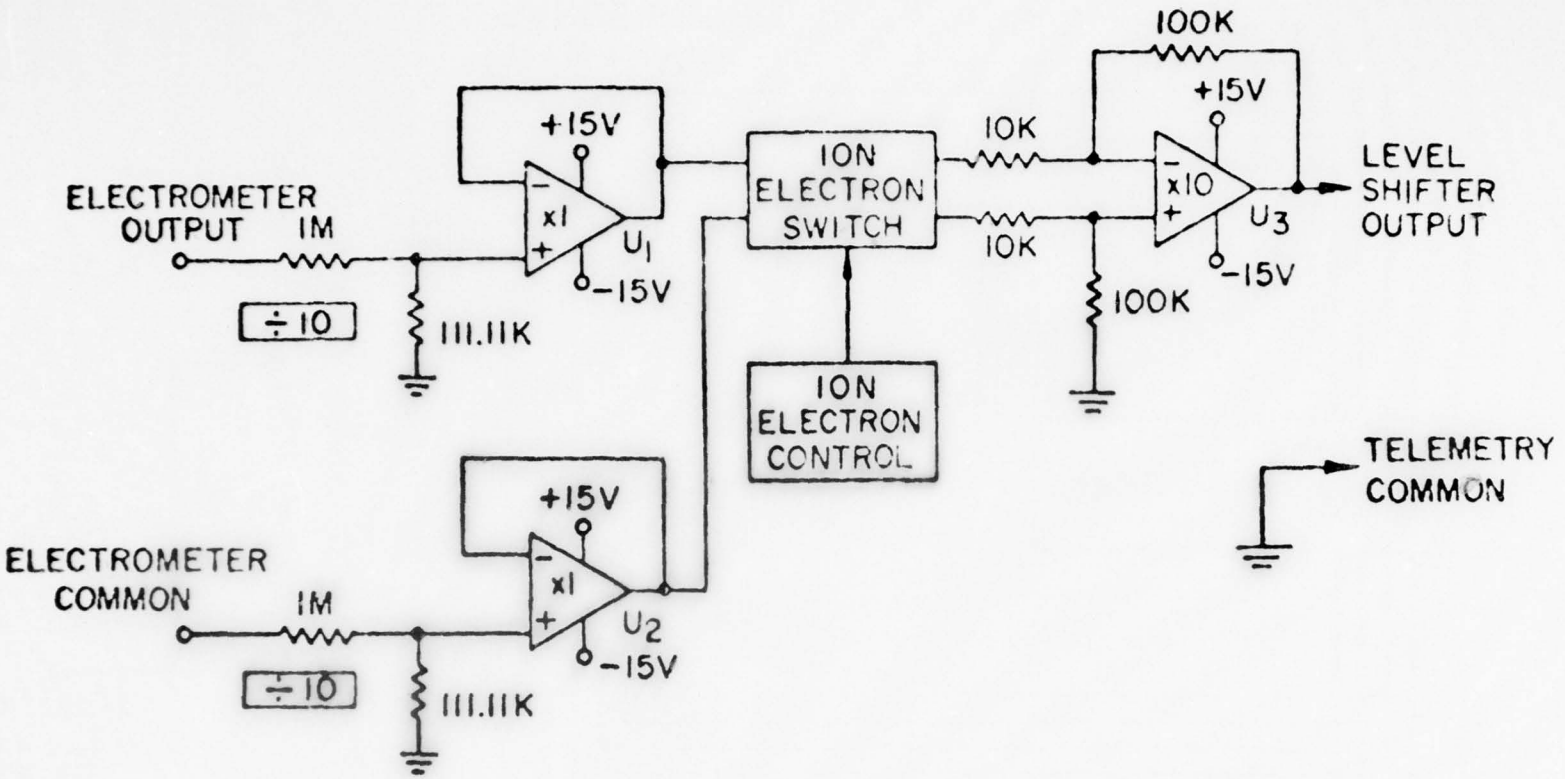

Figure 9. SCATHA level shifter circuit.

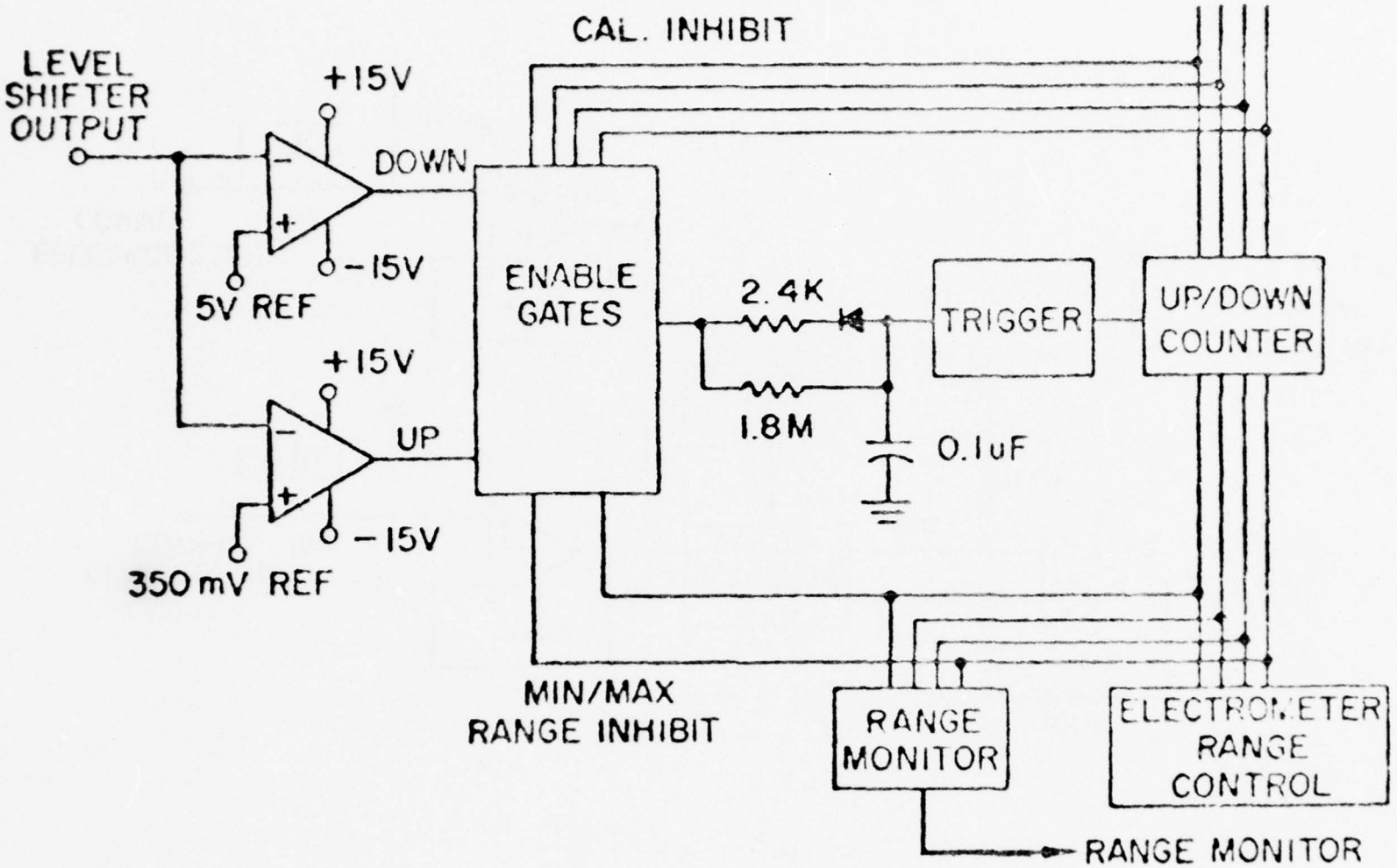

Figure 10. SCATHA automatic range-switching circuit.

4.5 STEP GENERATOR

Two step generators (ion and electron) are used for stepping the sensor grid elements and the electrometer floating common. One generator is applied in the electron modes and the other generator is applied in the ion modes.

4.6 TIMING AND CONTROL CIRCUITS

Timing of the system program is clocked from a spacecraft-provided 1-Hz pulse. The system program cycle is approximately 1 hour long. The cycle is achieved by using a 12-stage counter and a diode matrix as shown in Figure 11. The decoded lines from the matrix are used for controlling the electrometer calibration sequence and sweep periods. The system timed sequence of events is shown in Figure 12.

4.7 TELEMETRY OUTPUTS

The experiment data output lines are listed in Table 2. Each output is fed to a telemetry system consisting of an 8-bit Analog/Digital converter and a Pulse Coded Modulation (PCM) encoder.

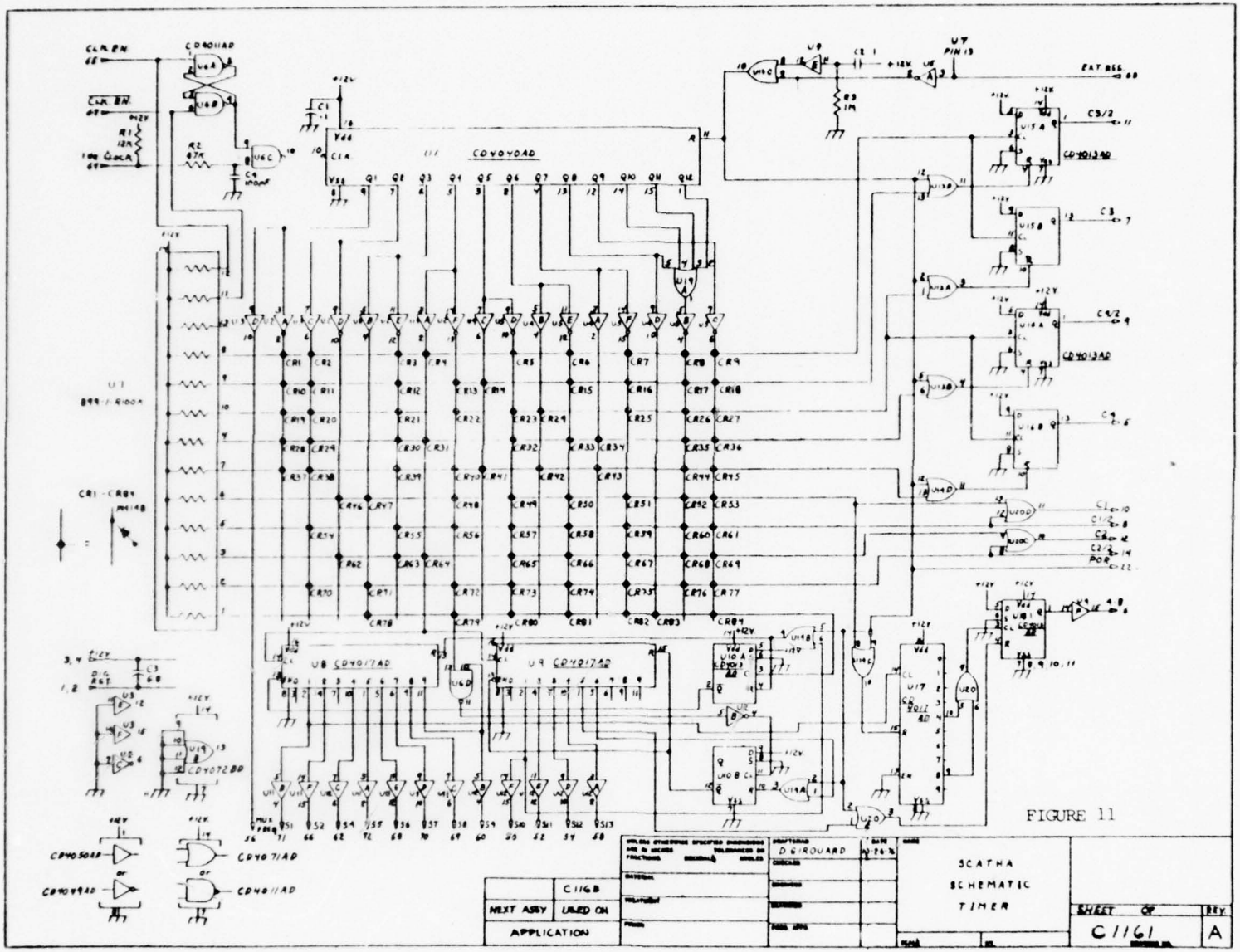
SCATHA
SCHEMATIC
TIMER
C1161
A
SHEET OF
C116B
NEXT ASSY
USED ON
APPLICATION
D GIROUARD

FIGURE 11

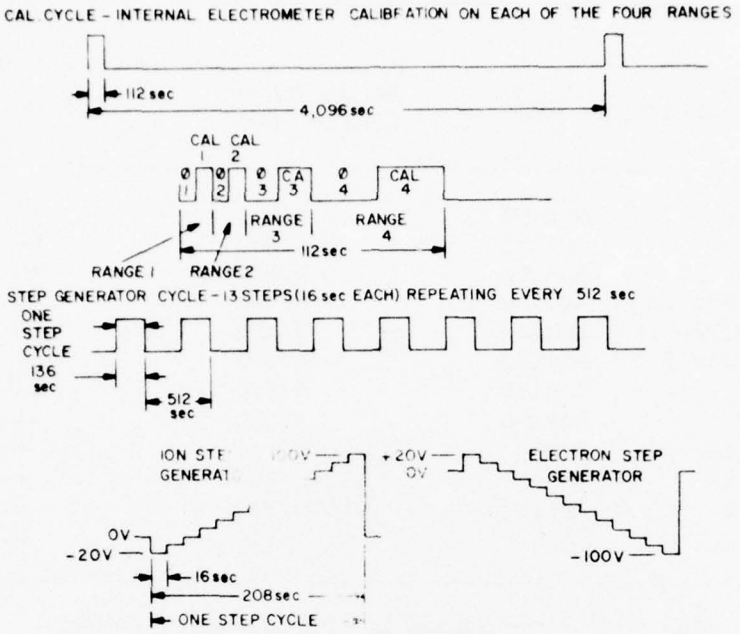

Figure 12. SCATHA system timed sequence of events

Table 2. SCATHA Data Output Lines.

TM Output Description	Type	Bandwidth or Sample Rate	Bits/sec
*Current Sensor 1A	Analog	8/sec	64
*Range/Cal Sensor 1A	Analog	8/sec	64
*Current Sensor 1R	Analog	8/sec	64
*Range/Cal Sensor 1R	Analog	8/sec	64
*Current Sensor 2	Analog	8/sec	64
*Range/Cal Sensor 2	Analog	8/sec	64
*Step Monitor	Analog	8/sec	64
Event Monitor	Analog	2/sec	16
Temp Monitor 1A	Analog	0.0625/sec	0.5
Temp Monitor 1R	Analog	0.0625/sec	0.5
Temp Monitor 2	Analog	0.0625/sec	0.5
Bias Monitor	Analog	0.0625/sec	0.5

*These output words to be contiguous in the telemetry format.

5. FIGURES AND TABLES CITED IN THE TEXT

ANALYSIS OF PLASMA AND FIELD MEASUREMENTS ABOARD THE INJUN 5, S3-2 AND S3-3 SATELLITES

WILLIAM J. BURKE

1. INTRODUCTION

This note is submitted as a final report on work accomplished by Dr. William J. Burke between 1 September 1975 and 30 April 1977. The bulk of the work concerns the analysis of plasma and field measurements by Air Force experiments aboard the Injun 5, S3-2 and S3-3 satellites. The purpose of these analyses is to increase our understanding of physical processes in the topside ionosphere and to develop suitable instrumentation for measuring low energy plasmas found at up to 7 earth radii (R_E). Using expertise developed in the fields of keV particle measurements, theoretical magnetospheric physics and microwave remote sensing, prior to joining the Regis College Research Center, I have spent approximately five percent of my time consulting, on an informal basis, with Air Force scientists in the Geomagnetism and Optical Physics branches of AFGL. The purpose of these consultations is to develop more integrated systems for the detection of particles and fields using instrumentation aboard Air Force satellites. Work concerned with each of the above described endeavors is outlined below.

2. INJUN 5 DATA REDUCTION AND ANALYSIS

The first three months of my work was given to doing rather fundamental library research concerning the theory of Langmuir probes, and familiarizing myself with previously reported measurements from the topside ionosphere. Between December 1975 and April 1976, I began an in-depth re-evaluation of the state of Injun 5 data reduction. Several serious errors, introduced by an unsuspected spurious ground command, were detected. Several months were spent in rewriting Injun 5 data reduction programs, done largely by S. C. Bredesen of AFGL. With these modifications, scientific analysis began.

The corrected Injun 5 data were used in four major and two subsidiary studies. These include:

(1) The interaction between polar cap and auroral zone precipitating particles and the topside ionospheric plasma.

(2) The effects of precipitation on the electric potential of a satellite near 2500 km.

(3) Direct measurements of the heating effects of energetic photoelectrons from the conjugate ionosphere or the nighttime topside ionosphere.

(4) Direct observations of plasma erosions from the topside ionosphere during an intense geomagnetic storm.

(5) A theoretical analysis of the response of a gridded spherical electrostatic probe (similar to that of Injun 5) to anisotropic or non-Maxwellian plasmas.

(6) The effects of secondary electron emissions on measurements by Injun 5 electrostatic analyzers.

The first two studies involved a comparison of simultaneous observations by AFGL low energy plasma detectors and those of the University of Iowa LEPEDEA experiment aboard Injun 5. A preliminary version of the first study was presented at the April 1, 1976, meeting of the American Geophysical Union. A more detailed study has been accepted for publication in the Journal of Geophysical Research (JGR) in 1977. (Cf. References 1 and 6.) The second study was presented at the Spacecraft Charging and Technology Conference sponsored by the Air Force and NASA. A paper based on this report has been published in the Proceedings of the conference. (Cf. Reference 4.)

Due to the tilt of the earth's axis with respect to the ecliptic plane and the offset between the geographic and geomagnetic poles, energy is exhanged between conjugate hemispheres. At the time of the

winter solstice, the southern ionosphere is most illuminated by the solar flux. It is possible for a point in the southern hemisphere to be in sunlight and its conjugate point in the northern ionosphere to be in darkness. Energetic photoelectrons generated above 250 km in the southern ionosphere have mean free paths greater than the ionospheric scale height and can escape along magnetic field lines to provide energy for the nighttime conjugate point. In Figure 1, we have plotted contours of constant solar zenith angle at 300 km in the conjugate ionosphere for given northern magnetic latitudes as functions of geographic longitude. The calculations assume that the longitude in question is at local midnight near the time of the winter solstice. These contours show that the deepest (in latitude) penetration of conjugate photoelectrons occurs over the western Atlantic-central North American longitude section. No conjugate photoelectrons should be observed in the Asian longitude sector. Because there is a heat source available to north American but not Asian mid-latitudes, the ionospheric scale heights measured over the United States will be greater than those found over the U. S. S. R. An example of the heating effects of conjugate photoelectrons is given in Figure 2, where we have plotted the electron temperatures (T_e) and densities observed by Injun 5 during quiet time passes over central Siberia (orbit #1325) and over the western part of the United States (#1331). The satellite was at 2500 km in both instances. High electron temperatures are found in the trough in both the eastern and western hemispheres. Equatorward of the trough, T_e drops to about 2300 ^{o}K over Siberia, but maintains a value = 4000 ^{o}K over the United States until the conjugate solar zenith angle becomes greater than 105^{o}. For higher conjugate solar zenith angles on #1331, T_e falls to a value comparable to that found at sub-trough latitudes on #1325. A preliminary report on this study was presented orally at the International Symposium

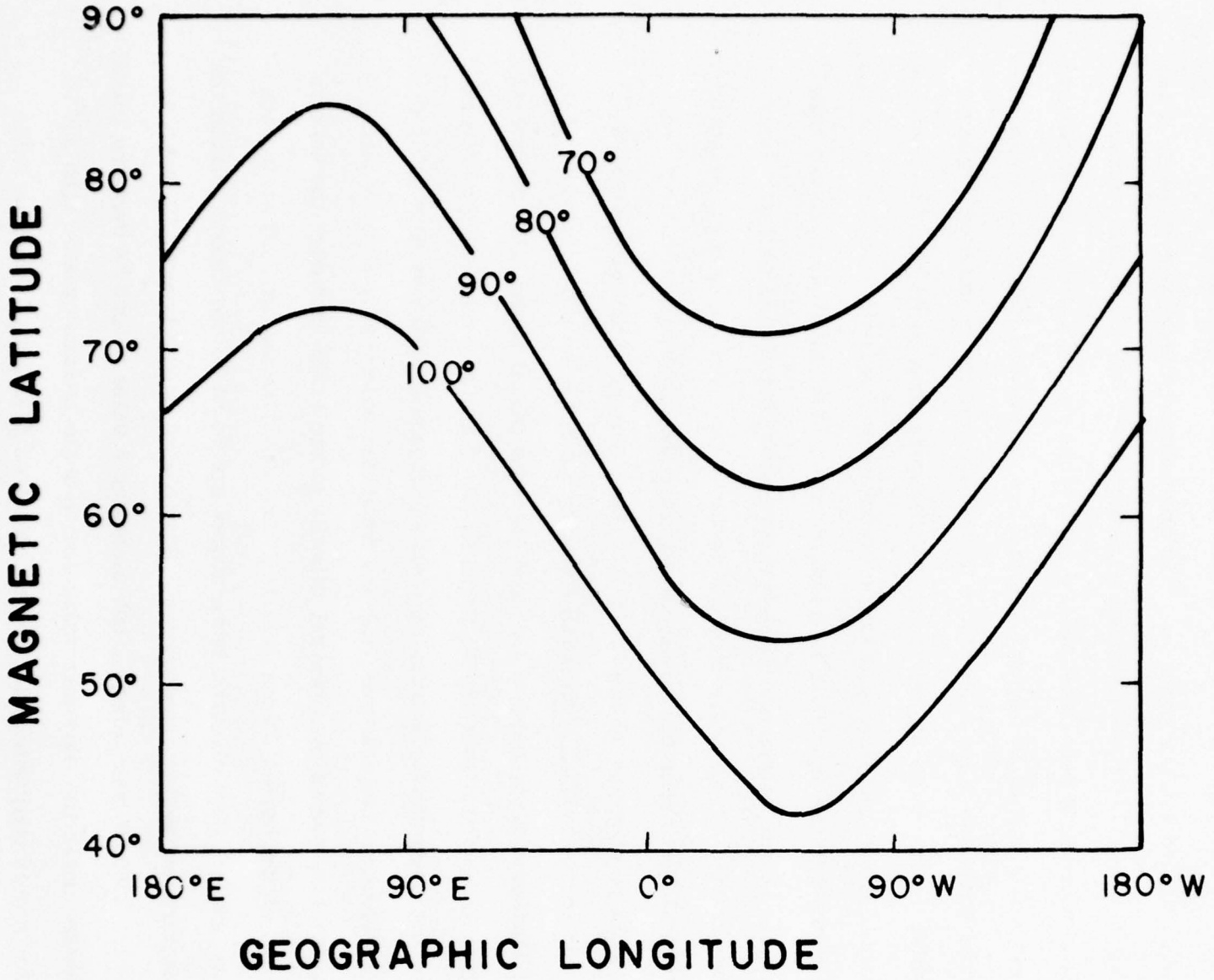

Figure 1. Contours of constant conjugate solar zenith angle at 300 km for given geomagnetic latitude as functions of geographic longitude. Calculations were made assuming that the meridian in question was near local midnight at the time of the winter solstice.

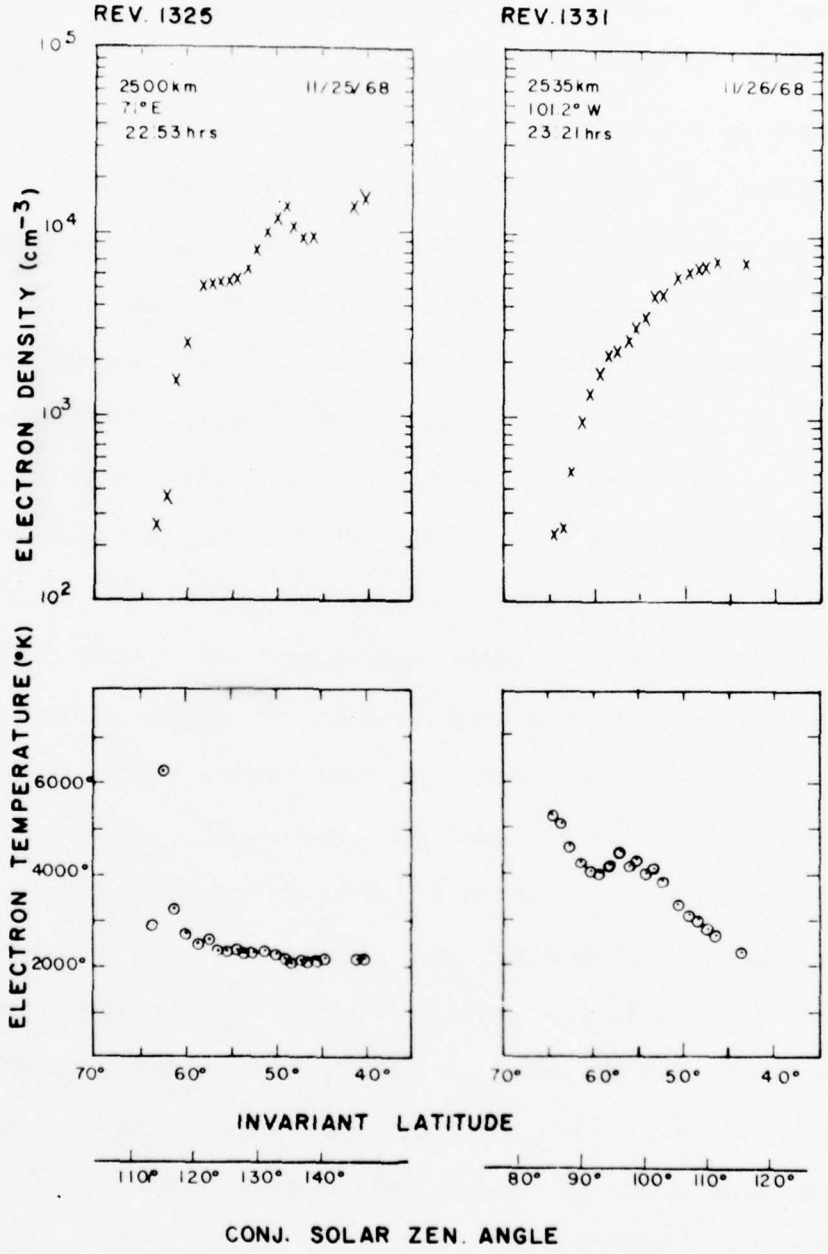

Figure 2. Electron densities and temperatures observed near 2500 km during Injun 5 orbits #1325 (over Central Asia) and #1331 (over Central North America) as functions of invariant latitude (Λ) and conjugate solar zenith angle. The altitude, longitude and local time of the satellite at $\Lambda = 60^{\circ}$ are indicated.

on Solar-Terrestrial Physics (Boulder, Colorado, June 1976). A more detailed study will be presented at the 1977 Spring Annual Meeting of the AGU. A written version has been submitted for publication in the Journal of Geophysical Research. (Cf. References 3, 9 and 11.)

When Dr. L. Rao was leaving the Research Center in the fall of 1976, the suggestion was made that I finish her work on the major magnetic storm of 29 October - 6 November 1968. Injun 5 was in the late evening local time sector and had fairly good coverage of the storm. Of particular interest to the scientists modelling the topside ionosphere is the ionospheric response to prolonged geomagnetic activity. The D_{st} history of the storm is outlined in Figure 3. Times of Injun 5 orbits and observed SAR activity are indicated. The electron densities observed at invariant latitude (Λ) of 60°, 55°, . . ., 40° as functions of universal time (UT) throughout the storm are given in Figure 4. Orbits #991 and #992 occurred just prior to the storm's sudden commencement and provide the quiet time ionospheric base. All data were taken in the altitude range $2000 \leq h \leq 2400$ km over the North American longitude sector. We note that whereas the density at 60° and 55° immediately responded by decreasing densities, the density remained unaffected for several days below these latitudes. We note that by the fourth day of the storm, density erosion occurred even at $\Lambda = 40^{\circ}$, This observation implies that the magnetospheric electric field was able to penetrate through the reported position of the plasmapause during the storm. A detailed study of the Injun 5 observations has been submitted for publication in the Journal of Geophysical Research. (Cf. Reference 7.)

The theoretical study on the response of gridded spherical electrostatic probes to non-Maxwellian plasmas was motivated by the knowledge that frequently distributions found above the ionosphere have "student-t"

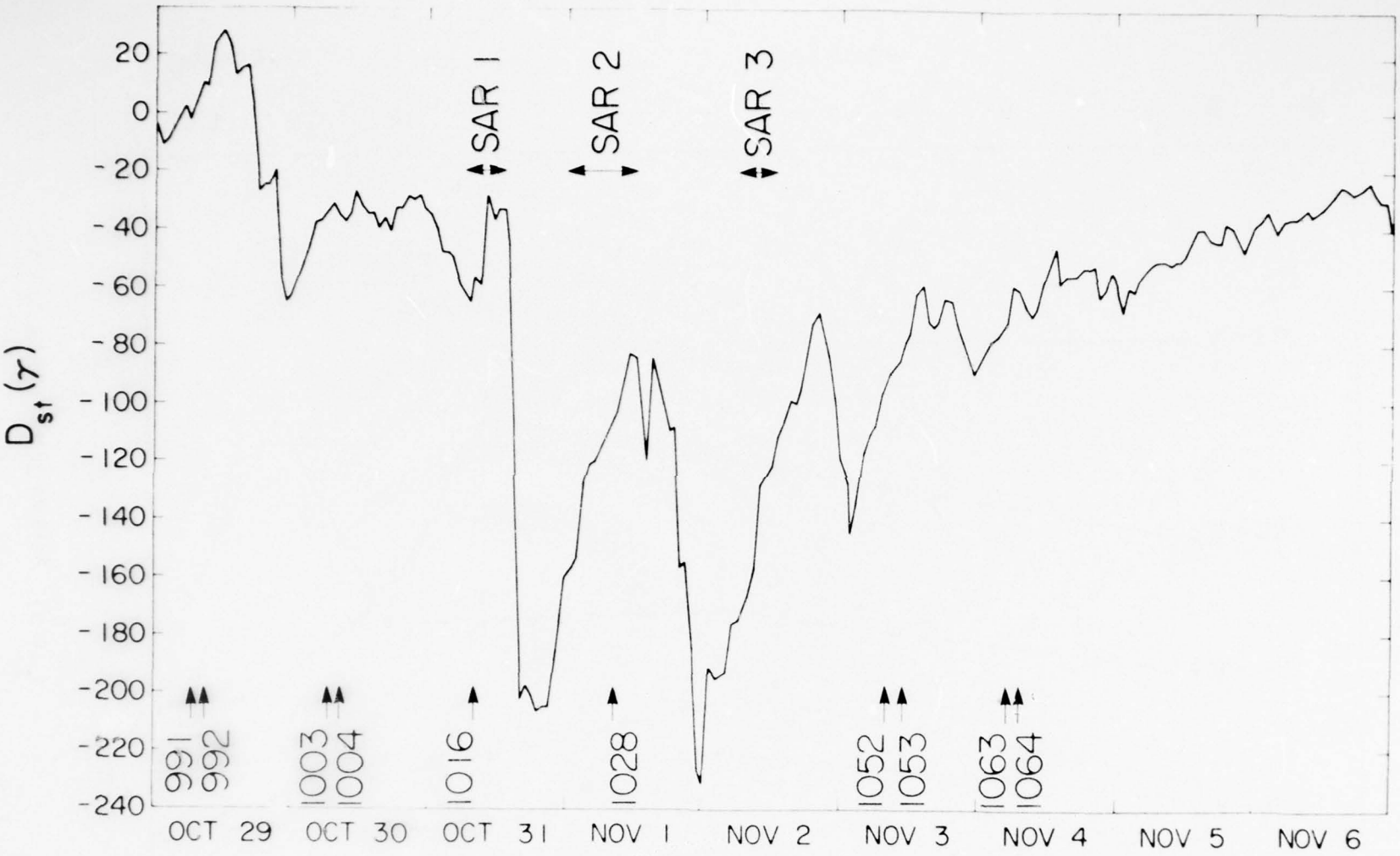

Figure 3. The D_{st} history of the October-November 1968 geomagnetic storm. Injun 5 orbits from which we have data are marked.

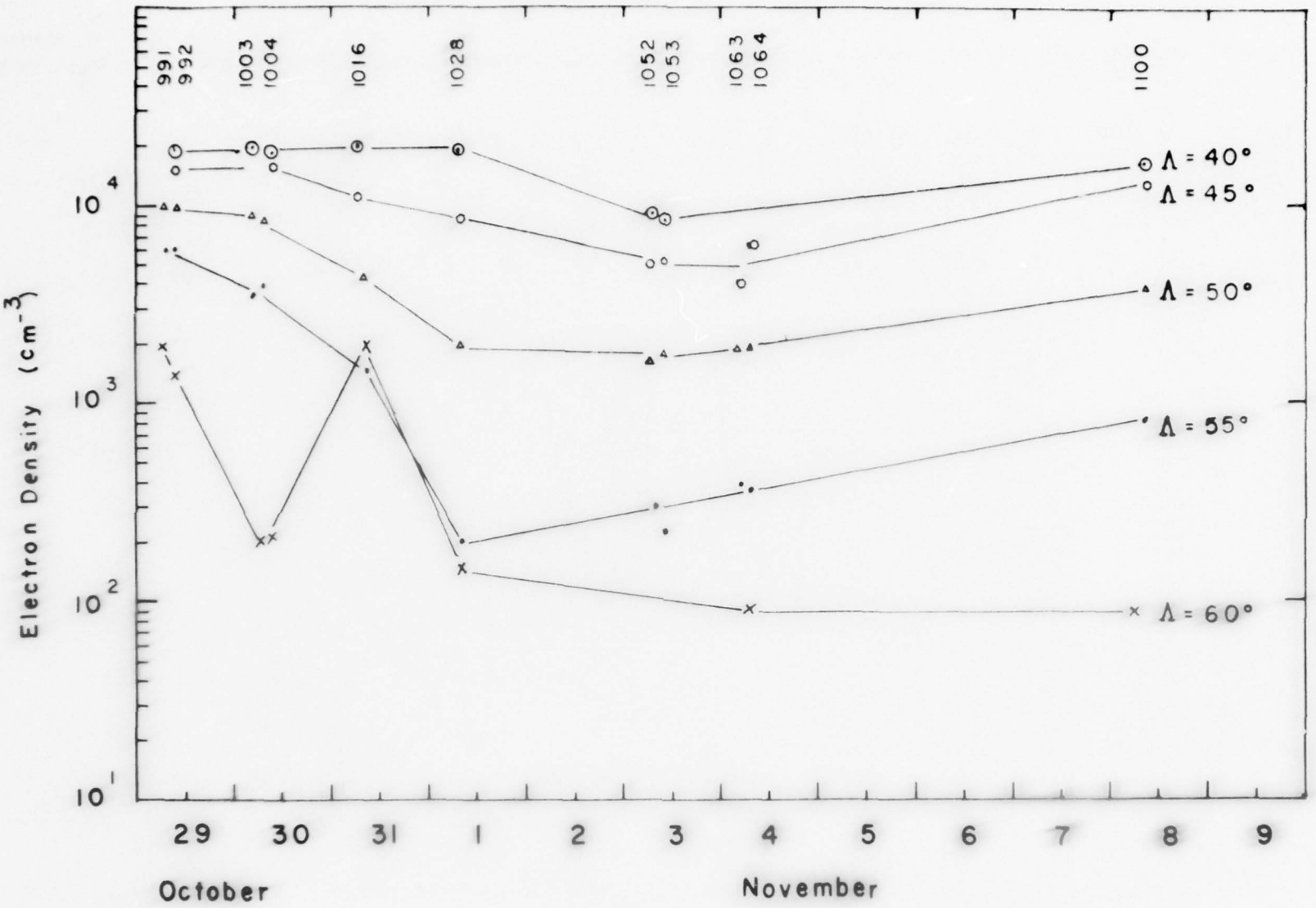

Figure 4. Electron densities observed at various invariant latitudes by Injun 5 as functions of universal time through the October-November 1968 geomagnetic storm.

rather than gaussian shapes. This study showed that with Injun 5 type instrumentation it is not possible to use current vs. applied grid voltage curves to distinguish the two type distributions. It was shown that mistaking a "student-t" distribution for a gaussian led to an overestimate of the electron density and mean thermal energy. The instrumentation planned for SCATHA, however, should be capable of distinguishing the two type distributions if the signals are above the amplifier's level of sensitivity. Such conditions should be met when SCATHA is inside the plasmasphere.

During September 1976, R. C. Sagalyn of AFGL received a first draft of a paper on Injun 5 observations from the Max Plank Institut für Aeronomie for comment and review. Since the work substantively overlapped what I was doing, she suggested that we undertake a collaborative endeavor. As a result, one and one-half months were spent analyzing the Injun 5 data referred to and studying the effects of secondary electron emissions from the Injun 5 instruments. A first draft of an internal report on secondary emissions was completed and a detailed critique of the work of the German scientists was returned to them. It is likely that within a year's time, a publishable report will come out of this work. We also believe that the time spent learning the theory of secondary electron emissions will pay rich dividends during the analysis of SCATHA data.

A review of my work on Injun 5 data was presented as an AFGL/PH seminar on 13 January 1977 for the benefit of Air Force scientists. (Cf. Reference 13.)

3. S3-2 AND S3-3

It was understood that during the period of Injun 5 analysis, I would also be available for consultation and some analysis of S3-2 and S3-3 data. Before Dr. F. J. Rich joined the group and assumed control of the plasma flow data analysis, I spent approximately one man-month assisting Dr. P. Wildman of AFGL in the preliminary stages of S3-2 data reduction. I have also spent time as a consultant to Dr. M. Smiddy of AFGL on the analysis of data from the S3-2 electric field experiment. We have finished the analysis of a magnetic storm during May, 1976 when intense electric fields were observed at the plasmapause and at the time and place of an observed SAR arc. This research will be presented at the 1977 spring annual meeting of the AGU. A detailed report will be submitted to Geophysics Research Letters for publication. Further analyses of the magnetic storm electric field observations of S3-2 are planned for the summer of 1977. (Cf. References 10 and 12.)

4. OTHER AIR FORCE RELATED ACTIVITIES

An informal relationship has been established between myself and Lt. D. Hardy (USAF) of the Geomagnetism Branch of AFGL. Both of us have prior experience analyzing plasma data observed by means of Apollo instruments on the surface of the moon. A preliminary study entitled "Plasma Mantle Observations at 60 R_E" is in the final stages for submission to the Journal of Geophysical Research for publication. Further studies of observations in the high latitude lobes of the geomagnetic tail will be undertaken. We have found evidence, based on spectral characteristics, that the tenuous plasma observed at the Moon is the same as that bombarding the polar cap ionosphere. This would provide a direct link between the distant magnetotail and the polar cap ionosphere. It would also provide a direct

measure of the energy available to maintain the night-time polar cap ionosphere. (Cf. Reference 14.)

Before coming to the Research Center, I was a National Research Council Fellow at Johnson Space Center studying the effects of soil moisture on the microwave emissions of natural terrains. On this basis, I have established an informal consulting relationship with V. Falcone of the Optical Physics Division. Instruments similar to those with which I have worked on NASA aircraft are to be flown on Air Force DMSP satellites. Our aim has been to make the best use of NASA experimental results for the development of interpretative algorithms for future Air Force passive microwave data. Since coming to Regis College, I have on my own time, contributed to the NASA technical note on microwave remote sensing. Another article on the same subject has been submitted for publication in the Journal of Geophysical Research. (Cf. References 2 and 8.)

5. REPORTS AND PAPERS

This section contains a list of oral reports and written papers. The abstracts of the reports are in section III-6.

1. Burke, W. J., R. C. Sagalyn, D. D. DuLong: Injun 5 observations of low energy electrons in the evening sector topside ionosphere, Trans. Amer. Geophys. U., 57, 307, 1976.
2. Schmugge, T. J., B. J. Blanchard, W. J. Burke, J. F. Paris and J. R Wang: Results of soil moisture flights during April 1974, NASA Technical Note D 8199, 1976.
3. Burke, W. J., M. Kanal and R. C. Sagalyn: On the heating of plasma trough electrons, presented at the International Symposium on Solar-Terrestrial Physics, Boulder, Colorado, June 7 - 18, 1976.
4. Sagalyn, R. C. and W. J. Burke: Injun 5 observations of vehicle potential fluctuations at 2500 km, Proc. Spacecraft Charging Technology Conference, ed. C. P. Pike and R. R. Lovell, AFGL-TR-77-0051, USAF Academy, Colorado Springs, Colorado, October 27 - 29, 1976.
5. Burke, W. J.: A model for inverted-V precipitation originating in the magnetosphere, Trans. Amer. Geophys. U., 57, 989, 1976.
6. Burke, W. J., D. D. DuLong and R. C. Sagalyn: Injun 5 Observations of low-energy plasma in the high-latitude topside ionosphere, J. Geophys. Res., 82, 1977 (to be published).
7. Rao, L. D. V., W. J. Burke, M. Kanal and R. C. Sagalyn: Injun 5 low-energy plasma observations during a major magnetic storm, (submitted to J. Geophys. Res., 1977).
8. Burke, W. J., T. J. Schmugge and J. F. Paris, Direct Observation of soil moisture by microwave radiometric techniques, (submitted to J. Geophys. Res., 1977).

9. Burke, W. J. and R. C. Sagalyn: Direct observations of conjugate photoelectron heating in the winter night-side ionosphere, Trans. Amer. Geophys. U., 58, 1977 (in press).

10. Smiddy, M., M. C. Kelley, R. C. Sagalyn, P. J. L. Wildman, B. M. Shuman, W. J. Burke, F. J. Rich, R. Hayes and S. T. Lai: Sub-auroral electric field observations during a magnetic storm, Trans. Amer. Geophys. U., 58, 1977 (in press).

11. Burke, W. J., R. C. Sagalyn and M. Kanal: Thermal and hyperthermal electron distributions in the midnight sector of the winter topside ionosphere (submitted to J. Geophys. Res., 1977).

12. Smiddy, M., M. C. Kelley, W. J. Burke, F. J. Rich, R. C. Sagalyn, B. M. Shuman, R. Hayes and S. T. Lai: Intense poleward-directed electric fields near the ionosphere projection of the plasmapause (to be submitted to Geophys. Res. Lett., 1977).

13. Burke, W. J.: Injun 5 low-energy plasma observations in the winter ionosphere, AFGL/PH seminar, January 13, 1977.

14. Reiff, P. H., D. A. Hardy and W. J. Burke: Plasma mantle observations at 60 R_E, (to be submitted to J. Geophys. Res., 1977).

6. REFERENCED ABSTRACTS

1. INJUN-5 OBSERVATIONS OF LOW ENERGY ELECTRONS IN THE EVENING SECTOR TOPSIDE IONOSPHERE

The polar orbiting Injun-5 satellite is equipped with two spherical electrostatic analyzers measuring currents produced by thermal and hyperthermal electrons and ions with energies in excess of 28 eV. We report on observations made by these instruments over the altitude range 2000-3000 km near 20:00 LT. The current characteristics observed in the quiet time polar cap region show consistent electron densities and temperatures of $\sim 1000\ cm^{-3}$ and $\sim 2000\ ^{o}K$. Auroral zone observations are reported in conjunction with the Iowa State LEPEDEA E-t spectrograms to identify "inverted V" signatures and the effects of precipitation. These effects include: (1) The production of ionospheric density and thermal irregularities and (2) rapid variations in the spacecraft potential. The equatorial boundary of the precipitation region is marked by a plasma with two distinct thermal electron populations. These relax to a single Maxwellian distribution at lower latitudes.

2. RESULTS OF SOIL MOISTURE FLIGHTS DURING APRIL 1974

The results presented here are derived from measurements made during the April 5 and 6, 1974 flights of the NASA P-3A aircraft over the Phoenix, Arizona agricultural test site. The purpose of the mission was to study the use of microwave techniques for the remote sensing of soil moisture. These results include infrared (10- to 12-μm) 2.8-cm and 21-cm brightness temperatures for approximately 90 bare fields. These brightness temperatures

are compared with surface measurements of the soil moisture made at the time of the overflights. These data indicate that the combination of the sum and difference of the vertically and the horizontally polarized brightness temperatures yield information on both the soil moisture and surface roughness conditions.

3. ON THE HEATING OF PLASMA TROUGH ELECTRONS

Current characteristics of a spherical electrostatic analyzer aboard the polar orbiting Injun 5 satellite have been used to study the plasma properties of the evening sector plasma trough's poleward boundary in the altitude range 2000-2500 km. It is found that the plasma is marked by two distinct electron populations which relax to a single Maxwellian distribution at lower latitudes. A linear regression analysis of the temperature of the thermal portion of the boundary layer electron population as a function of the hourly average of the auroral electrojet (AE) index shows that

$$Te \approx 4755 + 6.04 \cdot AE$$

with a correlation coefficient of ~ .9. These observations suggest that the trough region serves as a thermal sink for heat deposited in the auroral ionosphere by precipitating magnetospheric particles. The relative merits of various heat transport mechanisms are discussed.

4. INJUN 5 OBSERVATIONS OF VEHICLE POTENTIAL FLUCTUATIONS AT 2500 KM

The AFGL spherical electrostatic analyzers aboard the polar orbiting Injun 5 satellite were designed to measure the temperature and density of the plasma as well as the vehicle potential. Significant vehicle potential fluctuations have been observed at altitudes

near 2500 km in the night-time, topside ionosphere. At auroral latitudes, precipitating magnetospheric electrons frequently drive the satellite to such strongly negative potentials that the ambient electrons are shielded from our instruments. In such cases simultaneous measurements by the Iowa State University LEPEDEA experiment can be used to calculate the vehicle potential. Potentials of up to -40 volts are observed during impulsive precipitation events. Within the plasma trough, vehicle potentials vary between -1.5 and -4 volts, as compared with the -0.5 to -1 volt observed in the polar cap. The source of this vehicle potential enhancement is ascribed to fluxes of photoelectrons that have escaped from the sunlit conjugate ionosphere.

5. A MODEL FOR INVERTED V PRECIPITATION ORIGINATING IN THE MAGNETOSPHERE

Simultaneous observations by the AFGL spherical electrostatic analyzer and the University of Iowa LEPEDEA aboard the polar orbiting Injun 5 satellite suggest a magnetospheric origin for evening sector 'inverted V' precipitation. We attempt to synthesize these with plasma observations in the distant portions of the magnetotail. A magnetospheric model is presented following Vasyliunas' suggestion that at great distances from the earth, the plasma sheet is bound by a slow mode wave emanating from the merging region. It is shown that if the earthward flow of plasma is obstructed by a magnetic bottle in the neutral sheet, many qualitative features of inverted V structures may be accounted for. These include: (1) A sharp high latitude turn on for structured, field-aligned precipitation; (2) a position for some structures poleward of the high energy electron 'trapping boundary';

(3) proximity to a reversal in the ionospheric electric field; and (4) homogeneous precipitation near the equatorward boundary.

6. INJUN 5 OBSERVATIONS OF LOW ENERGY PLASMA IN THE HIGH-LATITUDE TOPSIDE IONOSPHERE

The two Air Force Geophysics Laboratory (AFGL) low-energy spherical electrostatic analyzers aboard Injun 5 have provided observations which are used on conjunction with simultaneous LEPEDEA observations to study the energetic and ambient thermal plasmas in the evening sector topside ionosphere. Significant thermal electron flux enhancements are observed in the vicinity of the inverted-V structures which could be due to either auroral return currents or ionospheric scale-height changes. Enhanced hyperthermal ($E > 28$ eV) fluxes of positive ions, as well as vehicle potential modulations, are as the satellite passes through inverted V events. At 2500 km, the polar cap electron density, temperature and energy density were 89 ± 41 cm^{-3}, 2234 ± 480 ^{o}K and 16.2 ± 5.8 eV/cm^{3}, respectively. Higher energy densities are found during times of magnetic disturbance. Persistent fluxes of hyperthermal electrons are identified with the polar rain observed with Isis 2 experiments. Finally, evidence is cited for the existence of small scale (20 km) precipitation events at or near the equatorward boundary for auroral electron precipitation.

7. INJUN 5 LOW-ENERGY PLASMA OBSERVATIONS DURING A MAJOR MAGNETIC STORM

Electron densities and temperatures as well as the omnidirectional flux of positive ions with $E > 28$ eV were measured by the spherical Langmuir probes aboard Injun 5 at altitudes greater than 2000 km during the October-November 1968 geomagnetic storm period. During

the early phases of the storm, the electron density in the trough decreased and the temperature increased. As the storm progressed, the position of the trough moved equatorward. Plasma erosion was observed to the invariant latitude of 40° during the early recovery phase. The latitude of the transition between light and heavy ion dominance also moved equatorward, but recovered at a slower rate than the position of the electron trough. Most of the hyperthermal ions measured near the trough were due to ring-current particles reaching to the satellite's altitude. The minimum electron densities in the trough were measured to be within 1° of latitude of the maximum ion flux. The maximum electron temperatures were observed several degrees equatorward of the maximum ion flux. At the reported time and latitude of an SAR arc, an electron temperature of about 4700 °K was observed, whereas in the absence of the ring-current, a temperature of about 2000 °K would be expected. The observations are also used to evaluate a method for calculating the position of ring current using magnetic fluctuations observed at ground level.

8. DIRECT OBSERVATIONS OF SOIL MOISTURE BY MICROWAVE RADIOMETRIC TECHNIQUES

An airborne experiment was conducted under NASA auspices to test the feasibility of detecting soil moisture by microwave remote sensing techniques over agricultural fields near Phoenix, Arizona, at midday of April 5, 1974, and at dawn of the following day. Extensive ground data were obtained from 96 bare, sixteen hectare fields. Observations made using a scanning (2.8 cm) and a non-scanning (21 cm) radiometer were compared with the predictions of a radiative transfer emission model. It is shown that:

(1) The emitted intensity of both wavelengths correlates best with the near surface moisture.

(2) The emitted intensity is largely independent of the surface roughness, while the degree of polarization is greatly affected.

(3) The slope of the intensity-moisture curves decreases in going from day to dawn.

(4) Increased near surface moisture at dawn is characterized by increased polarization of emissions.

The results of the experiment indicate that microwave techniques can be used to observe the history of the near surface moisture. The subsurface history must be inferred from soil physics models which use microwave results as boundary conditions.

9. DIRECT OBSERVATIONS OF CONJUGATE PHOTOELECTRON HEATING IN THE WINTER, NIGHT-SIDE IONOSPHERE

We report on observations from the Injun 5 Langmuir probe experiment, of thermal the hyperthermal electron fluxes in the midnight sector of the northern winter ionosphere at altitudes between 2500 and 1000 km. It is found that the hyperthermal fluxes observed at mid-latitudes, with energies greater than 2 eV, result from photoelectrons that have escaped from the sunlit southern hemisphere. Due to the offset between the geographic and geomagnetic poles these photoelectrons are observed along orbits over the Atlantic Ocean and North America but not over Asia. At altitudes above 1000 km the highest electron temperatures are generally observed in the trough at all longitudes. Equatorward of the trough, however, electron temperature distributions are

functions of longitude. In regions of the topside ionosphere to which conjugate photoelectrons have access, the electron temperature is ~ 4200 ^{O}K for altitudes between 2200 and 2500 km and is ~ 3000 ^{O}K for altitudes between 1000 and 1200 km. In mid-latitude regions to which conjugate photoelectrons do not have access, the electron temperature is ~ 2300 ^{O}K over the entire altitude range.

10. SUB-AURORAL ELECTRIC FIELD OBSERVATIONS DURING A MAGNETIC STORM

Electric field observations from a two axis dipole system flown on the polar orbiting, spin stabilized, Air Force satellite S3-2 reveal the existence of intense local electric fields perpendicular to the magnetic field equatorward of the auroral oval. The events were detected in the evening sector near the ionospheric projection of the plasmapause during the magnetic storm of 1 - 3 May 1976. In one example, which we believe to be the largest electric field ever observed at low altitudes, the field was 280 mv/m, directed toward magnetic north at an altitude of 1460 km with a hundred kilometer latitudinal extent. These observations together with simultaneous ion drift and magnetic field measurements are used to deduce the local ionospheric current system.

11. THERMAL AND HYPERTHERMAL ELECTRON DISTRIBUTIONS IN THE MIDNIGHT SECTOR OF THE WINTER TOPSIDE IONOSPHERE

A gridded spherical electrostatic analyzer aboard Injun 5 has been used to measure fluxes of thermal and hyperthermal electrons at sub-auroral altitudes in the midnight sector of the northern ionosphere between altitudes of 2500 and 850 km. Hyperthermal fluxes, consisting of energetic photoelectrons that have escaped from the

sunlit southern hemisphere are observed along orbits over the Atlantic Ocean and North America but not over Asia. The electron temperatures near 2500 km have their highest values at trough for all longitudes. In the longitude sector to which conjugate photoelectrons have access, $T_e \sim 4000\ ^{o}K$ at 2500 km and $\sim 3000\ ^{o}K$ at 1000 km. For regions with the conjugate point in darkness $T_e \simeq 2300\ ^{o}K$ over the 1000-2500 km altitude range. Effective spectral characteristics of the photoelectrons are studied as functions of latitude and altitude. Based on these observations, it is concluded that: (1) Conjugate photoelectrons are not the major contributors to trough heating; (2) Heat conduction rather than local heating by conjugate photoelectrons is responsible for electron temperature distributions observed in regions with sunlit conjugate points.

12. INTENSE POLEWARD-DIRECTED ELECTRIC FIELDS NEAR THE IONOSPHERIC PROJECTION OF THE PLASMAPAUSE

The dc electric field experiment on the Air Force satellite S3-2 has occasionally detected intense localized electric fields near the ionosphere projection of the plasmapause. The field was poleward in the premidnight local time sector, seemed to be related to substorm activity and ofttimes exceeded 100 mV/m. A possible source is field-aligned currents associated with freshly injected plasma generated in the substorm process near magnetic midnight.

13. INJUN 5 LOW ENERGY PLASMA OBSERVATIONS IN THE WINTER IONOSPHERE

The two AFGL spherical analyzers (SEA) aboard the polar orbiting Injun 5 satellite were designed to measure the temperature and

density of thermal electrons, the omnidirectional flux of ions with energies greater than 28 eV and the satellite potential. We present a rather broad overview of observations taken from the late evening-midnight sector near the winter solstices of 1968 and 1969. Topics of particular interest include:

1. Spacecraft potential fluctuations during intense precipitation events.
2. Direct observations of the degree of ionospheric heating due to conjugate photoelectrons.
3. Using the secondary emissive properties of the instrument's materials as rough estimators of the mean atomic mass.

14. PLASMA MANTLE OBSERVATIONS AT 60 R_E

From an analysis of particle and field data taken during a major magnetic storm, we have determined several important features of the particle populations observed at lunar distance. First, by analysis of the time delay between the onset of the storm with the associated tail compression, and the observation of variation in the characteristics of the plasma mantle, we have inferred a near-earth source for these particles, most likely the cusp. Second, the electrons in the plasma mantle display a "core" and "halo" as do the solar wind and magnetosheath electrons, implying a solar wind source for the mantle. Third, the storm produces major changes in the plasma sheet. Prior to the storm onset, the plasma sheet is static with ion temperatures from $KT_i \sim 150$ to 400 eV.

7. FIGURES CITED IN THE TEXT

THE POLAR WIND EXPERIMENT

FREDERICK J. RICH

1. THE POLAR WIND EXPERIMENT is an array of four planar ion sensors set to observe the flux from directions separated by 40^{o} from one another. The experiment was designed and built by the Air Force Geophysics Laboratory, Electrical Processes Division. Two arrays were flown on the Air Force satellite S3-2, launched December 1975 into a 250 by 1550 km polar orbit, and one array was flown on the Air Force satellite S3-3, launched July 1976 into a 250 by 8000 km polar orbit. The arrays are mounted on these spin stabilized so that the normals to two sensors in each array are approximately in the spin plane. The other two normals are 40^{o} above and below the spin plane.

The work to analyze the data from the polar wind has proceeded slowly. A series of problems has arisen from the fact that the design of the experiment is new in many respects. Planar plasma sensors with flat current collecting plates have been used for over half a century, but never before has an array of planar sensors been mounted on a satellite to detect the bulk motion of a plasma from the difference in current collected from the various look directions.

The formula developed prior to launch for the analysis of the ion data used a very simple calculation of the direction of current to planar sensor. This calculation assumed the ion mean thermal speed to be negligible with respect to the ram speed of the satellite and assumed the plasma flowed from 2π steradians into an infinite plane. When data became available it was immediately obvious that the simple calculations could not be used in the analysis of the data.

The satellites carrying the polar wind experiments go through regions of the ionosphere where O^{+} is the dominant ion and has a mean thermal speed of approximately 1200 meters per second to regions where H^{+} dominates and has a mean thermal speed of 4 kilometers per second or more. The satellite velocity ranges from 7 to 9 kilometers per second. Thus the mean thermal speed of the ions is never negligible. This means that the current to the

planar sensor varies with the angle from the ram direction by an amount related to the mean thermal speed as well as the angle from the ram. In order to find the true ram direction (satellite velocity plus bulk plasma velocity), the temperature must be determined.

An additional complication is the fact that the array of planar sensors is recessed into the satellite surface which causes the field of view of the sensors to be partially blocked by the satellite. The portion of the field of view of each sensor that is obstructed is not a simple symmetric shape and is different for each sensor. A method for approximately dealing with the field of view was developed and described in detail in an AFGL Technical Note, co-authored by Dr. Peter Wildman of AFGL published in 1977.

The method of data analysis that was determined to be necessary to account for the thermal speed of the ions and the geometry of the sensors is a curve fitting procedure. Model curves of sensor current versus vehicle attitude during the portion of the spin cycle when the array faces the ram are calculated as a function of the plasma mean thermal speed, bulk motion and density. The plasma parameters are varied until a "best" fit is found of the theoretical curve to the data. This procedure is done by a computer program that has been developed during the first two quarters of 1977.

The above method of data analysis has several potential problems: The computer time required to fit the data can become excessive. The algorithm assumes that the plasma parameters are constant over a period of approximately 4 seconds, which is not always true. The algorithm ignores other problems such as the finite size of the satellite, satellite charging problems and spacecraft-plasma interactions.

The computer time required to solve for the plasma parameters has been a prime consideration in the construction of the computer codes. The program has been made as efficient as possible without sacrificing accuracy and reliability. The result is a program that runs approximately in real time, i.e.,

approximately five minutes of computer time are required to process five minutes of data from this experiment. It would seem that the task of processing large quantities of data will require large quantities of computer time. For the moment, only small sections of data will be processed based on the quick look data file and other criteria.

Variation of plasma parameter during a 4-second period is a problem that must be lived with at this time. Some attempts have been made to smooth the data on the bases of density fluctuations that might be detected by a spherical electron temperature/density probe. The results have been very limited due to the discovery of an array of problems associated with the electron probe. The nature of these problems is currently under investigation. In general, density variations over 4 seconds of the satellite's flight are of minor importance to the analysis of the ion data except in the auroral oval where data analysis is presently impossible.

Problems such as the entrance of particles into the sensors from regions of space that would be excluded if the sensors were mounted on an infinite plane have been considered. So far, it has only been possible to determine that there is a problem but no method of dealing with the problem has been developed due to the extreme complexity of the problem. For example, it has been found that extra particles are drawn in when the swept voltage function of the electron probe drives the satellite potential highly negative. At the moment, data taken during the electron probe's sweep can be excluded, but nothing can be done about data taken when the satellite potential naturally goes negative. More work on this problem needs to be done in the future.

2. RESULTS FROM THE EXPERIMENT

Since so much effort has been spent on development of ways to interpret the data, only a very modest amount has been analyzed in detail. The two most notable pieces of analysis and interpretation are related to a SAR (Stable Auroral Red) arc event on May 3 - 5, 1976 observed by S3-2 and the

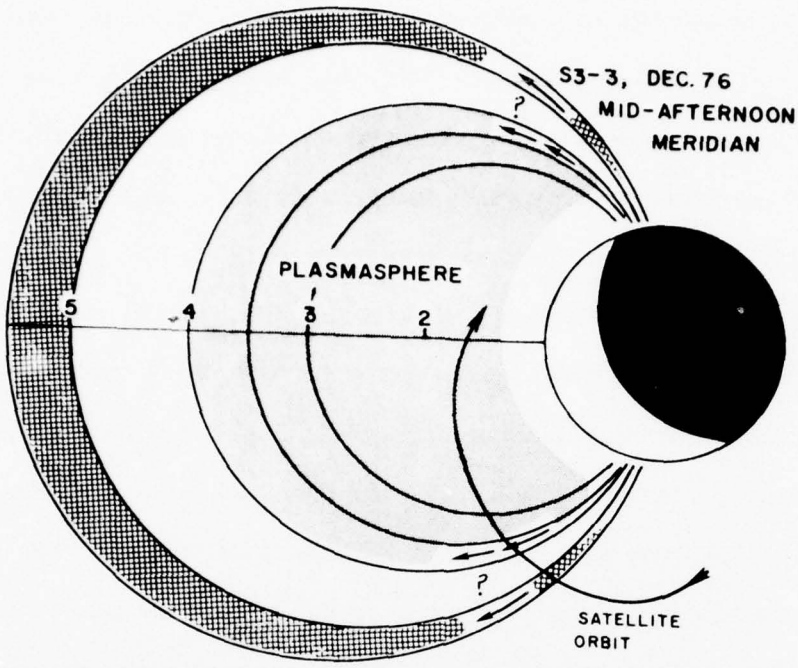

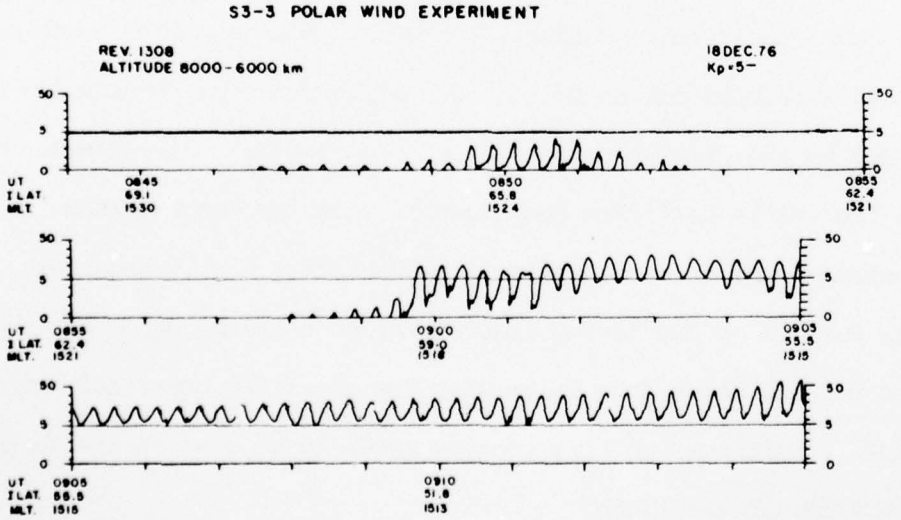

Figure 1. S3-3 December 1976 mid afternoon meridian; Polar Wind experiment.

passages through the plasmapause at high altitudes by S3-3.

The plasma in the ionosphere at the time and position of the SAR arc event was observed to be moving westward at a speed of 6 ± 3 km/s. This event was also detected by the AFGL electric field sensor on the S3-2 satellite. A complete analysis of this event is being done by other personnel and will be presented by Dr. Smiddy of AFGL at the Spring 1977 Meeting of the American Geophysical Union.

On the Air Force S3-3, with the use of the Polar Wind Experiment, we have been able to clearly define the location of the plasmapause when the satellite is above 3000 km altitude. Below this altitude other ionospheric effects tend to obscure the signature of the plasmapause. The most striking features found so far in the analysis of the ion data are (a) pronounced upward movement of ions at the plasmapause and several degrees equatorward of the boundary, and (b) a tendency, especially at geomagnetically disturbed times, for small segments of plasmasphere type plasma to reside a few degrees poleward of the plasmapause. This feature is shown in Figure 1. The upper portion of the figure is a schematic of the estimated arrangement of the plasma, and the lower portion shows the ion data for one S3-3 passage of the plasmapause. This work will be presented by myself at the Spring 1977 Meeting of the American Geophysical Union.

3. FUTURE SPACE MISSION

On an as-requested basis, I have provided analysis and suggestions on proposals and designs for future missions, being written by the Electrical Processes Division of AFGL. This work has mostly been related to space missions to be conducted from the NASA Space Shuttle.

The largest single piece of work in this area has been the development of a concept for an experiment to modify the ionosphere by injection of chemicals. The concept developed on this contract is to inject water (H_2O) into the ionosphere in a two-step process. First, the water will be released from the

Shuttle into a lower orbit. The water will be enclosed in a large balloon. The balloon will be filled with water vapor as the sunlight heats it. Then the water will be released from the balloon at the appropriate time. The advantages of this concept over those previously presented are: (a) placement of the modification of the ionosphere in front of, instead of behind, the Shuttle. The Shuttle with onboard instruments supplied by AFGL and others, will then be able to pass through the modification and measure it in situ; (b) A much greater percentage of the H_2O will be vaporized in a two-step method than is possible in a direct release of liquid H_2O into a vacuum (~20%). See Figure 2 for a detailed example of the results of a two-step procedure.

EQUILIBRIUM VAPOUR PRESSURE

MASS (H_2O) = 1000 kg, VOLUME = 12,000 m^3

Temperature °C	Vapour Pressure (mbar)	% Vapour
50	123.3	99.2
40	73.8	61 .2
30	42.9	36.8
20	23.7	21 .0
10	12.4	11 .4
0	6.0	5.7
-10	2.9	2.8
-15	1.9	1 .9

ADIABATIC VAPOURIZATION

ΔT °C	%Vapour
-10	1 .8
-20	3.7
-30	5.5
-40	7.4
-50	9.2

EXAMPLE:

1. $T_s = 20^\circ \longrightarrow T_d \approx -5^\circ$ C + 4.4% vapourized
2. Add heat $\longrightarrow T_e \simeq 33^\circ$ C with $\approx$ 40% vapourized
3. Open balloon $\longrightarrow$ 52% vapourized and 48% ice

Figure 2. Equilibrium vapour pressure; adiabatic vapourization.

4. SCIENTIFIC PUBLICATIONS OF RECENT RESEARCH

1. Frankel, J., F. J. Rich, C.G. Homan: Acoustic Velocities in Polycrystalline NaCl from 25 to 270 kbar, J. Geophys. Res., 1976.

2. Frankel, J. and F. J. Rich: Some considerations on the use of Sodium Chloride Isotropic Acoustic Velocity Ratio for Pressure Calibration, J. Appl. Phys. Letters, 1977.

3. Frankel, J., F. J. Rich, M. Hussain and R. D. Scanlon: Fourth Order Elastic Constants for Sodium Chloride to Pressures of 270 kbar, Bull. Am. Phys. Soc., 1977 (abstract).

4. Rich, F. J. and P. J. L. Wildman: Model for the Electrical Current Collected by a Planar Aperture Ion Collector with a Partially Blocked Field of View, AFGL-TR-77-0096, 1977.

5. Rich, F. J., R. C. Sagalyn, P. J. L. Wildman: Modification of the Ionosphere: A Proposed Method for Efficiently Injecting Water Molecules into the Ionosphere, EOS, 1977.

6. Wildman, P. J. L., R. C. Sagalyn and F. J. Rich, Ion Motion Measurements at High Altitudes from the S3-3 Satellite, EOS, 1977.

7. Frankel, J., F. J. Rich, C. G. Homan, The Use of the Sodium Chloride Isotropic Acoustic Velocity Ratio as a Calibration Parameter in Ultra-High Pressure Physics, Assoc. Internat. for Res. and Adv.of High Press. Sci. and Tech. Conf., 1977.

5. FIGURES CITED IN THE TEXT